

Department
of
APPLIED MATHEMATICS

A mathematical model for batch and continuous
thickening of flocculent suspensions in
vessels with varying section.

by

R. Bürger, J.J.R. Damasceno, and K.H. Karlsen

Report no. 159

October 2001



UNIVERSITY OF BERGEN
Bergen, Norway

Department of Mathematics
University of Bergen
5008 Bergen
Norway

ISSN 0084-778X

A mathematical model for batch and continuous
thickening of flocculent suspensions in
vessels with varying section.

by

R. Bürger, J.J.R. Damasceno , and K.H. Karlsen

Report no. 159

October 2001

NB Rana
Depotbiblioteket

A MATHEMATICAL MODEL FOR BATCH AND CONTINUOUS THICKENING OF FLOCCULENT SUSPENSIONS IN VESSELS WITH VARYING CROSS SECTION

R. BÜRGER^{A,*}, J.J.R. DAMASCENO^B, AND K.H. KARLSEN^C

ABSTRACT. The phenomenological theory of continuous thickening of flocculated suspensions in an ideal cylindrical thickener is extended to vessels having varying cross-section, including divergent or convergent conical vessels. The purpose of this contribution is to draw attention to the corresponding mathematical model, whose key ingredient is a strongly degenerate parabolic partial differential equation. For ideal (non-flocculated) suspensions, which do not form compressible sediments, the mathematical model reduces to the kinematic approach by Anestis, who developed a method of construction of exact solution by the method of characteristics. The difficulty lies in the fact that characteristics and iso-concentration lines, unlike the conventional Kynch model for cylindrical vessels, do not coincide, and one has to resort to numerical methods to simulate the thickening process. A numerical algorithm is presented and employed for simulations of continuous thickening. Implications of the mathematical model are also demonstrated by steady-state calculations, which lead to new possibilities in thickener design.

1. INTRODUCTION

In a series of papers it was shown that the phenomenological theory of sedimentation-consolidation processes provides a robust mathematical framework for modelling solid-liquid separation processes of flocculated suspensions, including batch and continuous thickening in cylindrical vessels (Bürger et al., 1999; Bustos et al, 1999), batch centrifugation (Bürger and Concha, 2001) and pressure filtration (Bürger et al., 2001). In this contribution we extend the theory to batch and continuous thickening in vessels with non-constant cross section. This application is of significant practical interest since most industrial thickeners have a conically shaped bottom (to facilitate sediment removal), and thickeners whose cross-sectional area varies substantially over the entire effective height ('deep cone thickeners') are known to operate more efficiently (i.e., occupy less volume and permit faster fill-up and transitions between steady states) than cylindrical ones.

This paper is organized as follows. In Section 2 we formulate the mathematical model, which can be expressed as a nonstandard strongly degenerate parabolic-hyperbolic partial differential equation for the local solids concentration together with initial and boundary conditions. We recall some basic results of the mathematical analysis of such equations and consider the special case of steady states, i.e. stationary solutions representing normal operating conditions of the continuous thickener. The steady state analysis is in the compression zone equivalent to previous work by Resende et al. (1995). In Section 3 we present a working finite difference numerical algorithm for the numerical solution of the partial differential equation and thus for the simulation of batch and continuous thickening in vessels with varying cross section. A numerical algorithm has to be used since even in the compression-free case, in which the model reduces to a first-order equation, it is

Date: October 8, 2001.

Key words and phrases. Sedimentation-consolidation process; flocculated suspension; boundary conditions; feed source; hyperbolic-parabolic equation.

^AInstitute of Mathematics A, University of Stuttgart, Pfaffenwaldring 57, D-70569 Stuttgart, Germany.
E-mail: buerger@mathematik.uni-stuttgart.de.

^BFaculty of Chemical Engineering, Federal University of Uberlândia, Av. João Naves de Ávila, 2160, bl. K, Campus Santa Mônica, 38408-222 Uberlândia, MG, Brazil.
E-mail: jjrdamasceno@ufu.br.

^CDepartment of Mathematics, University of Bergen, Johs. Brunsgt. 12, N-5008 Bergen, Norway.
E-mail: kenneth.karlsen@mi.uib.no .

*Corresponding author.

in general not difficult (unlike the cylindrical case) to construct weak solutions by the method of characteristics. To elucidate this problem we consider in Section 4 the sub-case of batch settling of an ideal (non-flocculated) suspension in a conical vessel and outline, following Anestis (1981), the basic transformations that have to be made to apply the method of characteristics. A collection of sample numerical solutions for ideal suspensions is presented.

Obviously, the steady-state analysis of the model of thickening in vessels with varying cross-section permits including the shape of a thickener as a new design factor, and the numerical algorithm of the time-dependent partial differential equation allows to simulate the dynamic behaviour of the thickener. This is demonstrated in Section 5 by two calculated stationary and transient examples. Thus a more systematic analysis similar to that of Tiller and Chen (1988) would be warranted. Conclusions that can be drawn from this paper are collected in Section 6.

2. MATHEMATICAL MODEL

2.1. Continuity equations. We consider a vertical settling vessel with a variable cross-sectional area $S(x)$, where $0 \leq x \leq L$ is the height variable. We assume that the volumetric solids concentration ϕ is constant across each horizontal cross-section, i.e. $\phi = \phi(x, t)$. Then the conservation of mass equation for the solids is given by

$$S(x) \frac{\partial \phi}{\partial t} + \frac{\partial}{\partial x} (S(x) \phi v_s) = 0, \quad 0 \leq x \leq L, t > 0, \quad (1)$$

where t is time and v_s is the solids phase velocity. The analogue conservation equation for the fluid reads

$$-S(x) \frac{\partial \phi}{\partial t} + \frac{\partial}{\partial x} (S(x) (1 - \phi) v_f) = 0, \quad 0 \leq x \leq L, t > 0, \quad (2)$$

where v_f is the fluid phase velocity. The mixture flux, that is the volume average flow velocity appropriately weighted with the cross-sectional area at height x , is given by

$$Q(x, t) := S(x) (\phi v_s + (1 - \phi) v_f). \quad (3)$$

The sum of (1) and (2) produces the continuity equation of the mixture,

$$\frac{\partial}{\partial x} Q(x, t) = 0, \quad 0 \leq x \leq L, t > 0. \quad (4)$$

Equation (4) implies that $Q(\cdot, t)$ is constant as a function of x . Since this quantity suffers no jump across a discontinuity of ϕ , we obtain that

$$Q(x, t) = Q(0, t) = Q_D(t), \quad 0 \leq x \leq L, t > 0, \quad (5)$$

where $Q_D(t) \leq 0$ is the prescribed signed volumetric suspension discharge rate at $x = 0$.

Equation (5) is equivalent to one of the mass balance equations. We let (5) replace the fluid mass balance equation (2) and rewrite the solids balance equation (1) in terms of the flow rate $Q_D(t)$ and the solid-fluid relative velocity or slip velocity $v_r := v_s - v_f$, for which a constitutive equation will be formulated. Observing that

$$\phi v_s = (\phi v_s + (1 - \phi) v_f) \phi + \phi(1 - \phi)(v_s - v_f) = \frac{Q_D(t)}{S(x)} + \phi(1 - \phi) v_r,$$

we obtain from (1) the equation

$$\frac{\partial \phi}{\partial t} + \frac{1}{S(x)} \frac{\partial}{\partial x} (Q_D(t) \phi + S(x) \phi(1 - \phi) v_r) = 0. \quad (6)$$

2.2. Closure relationship for the slip velocity. The well-known kinematic sedimentation theory by Kynch (1952) is based on the assumption that the solid-fluid relative velocity or slip velocity v_r is a function of the local solids concentration ϕ only, $v_r = v_r(\phi)$. The slip velocity is usually expressed in terms of the Kynch batch flux density function f_{bk} . In the framework of the kinematic theory we have

$$v_r(\phi) = \frac{f_{\text{bk}}(\phi)}{\phi(1 - \phi)}, \quad (7)$$

such that Eq. (6) takes the form

$$\frac{\partial \phi}{\partial t} + \frac{1}{S(x)} \frac{\partial}{\partial x} (Q_D(t)\phi + S(x)f_{\text{bk}}(\phi)) = 0. \quad (8)$$

The function f_{bk} is usually assumed to be piecewise differentiable with $f_{\text{bk}}(\phi) = 0$ for $\phi \leq 0$ or $\phi \geq \phi_{\text{max}}$, where ϕ_{max} is the maximum solids concentration, $f_{\text{bk}}(\phi) < 0$ for $0 < \phi < \phi_{\text{max}}$, $f'_{\text{bk}}(0) < 0$ and $f'_{\text{bk}}(\phi_{\text{max}}) \geq 0$. A typical example is due to Michaels and Bolger (1962):

$$f_{\text{bk}}(\phi) = u_{\infty} \phi (1 - \phi/\phi_{\text{max}})^C, \quad u_{\infty} < 0, \quad C \geq 1, \quad (9)$$

where u_{∞} is the settling velocity of a single floc in pure fluid. There exists a vast body of literature related to the determination of appropriate functions f_{bk} from theoretical insight (Davis and Acrivos, 1985), experiments (França et al., 1999; França, 2000; Garrido et al., 2000; Bürger et al., 2000a) and discrete simulation (Quispe et al., 2000).

The field equation of the kinematic model, Equation (8), is a first-order hyperbolic partial differential equation. As is well known, its solutions are in general discontinuous due to the propagation of the solution along characteristics, which are straight lines in the case $S \equiv \text{const}$. However, most suspensions are flocculent and thus form compressible sediment layers, which are characterized by curved iso-concentration lines and can therefore not be predicted by the kinematic theory. Rather, an extended dynamic model including the concepts of pore pressure and effective solids stress has to be used.

Such a model is provided by the phenomenological theory of sedimentation (Bürger et al. 1999, 2000d), which is based on the mass and linear momentum balance equations for the solid and fluid components. By introducing constitutive assumptions, performing a dimensional analysis and considering one space dimension only, this theory leads to the following equation for the relative velocity v_r , which plays the role of one of the linear momentum balances:

$$v_r = \frac{f_{\text{bk}}(\phi)}{\phi(1-\phi)} \left(1 + \frac{\sigma'_e(\phi)}{\Delta \rho g \phi} \frac{\partial \phi}{\partial x} \right), \quad (10)$$

where $\Delta \rho > 0$ denotes the solid-fluid density difference, g the acceleration of gravity and $\sigma'_e(\phi)$ is the derivative of the effective solid stress function $\sigma_e(\phi)$, which is the second constitutive function (besides f_{bk}) describing the material behaviour of the suspension. This function is assumed to satisfy $\sigma_e(\phi) \geq 0$ for all ϕ and

$$\sigma'_e(\phi) := \frac{d\sigma_e(\phi)}{d\phi} \begin{cases} = 0 & \text{for } \phi \leq \phi_c, \\ > 0 & \text{for } \phi > \phi_c, \end{cases} \quad (11)$$

where ϕ_c is the critical concentration or gel point at which the solid flocs start to touch each other.

2.3. Final form of the governing equation. Inserting (10) into (6) and defining

$$a(\phi) := -\frac{f_{\text{bk}}(\phi)\sigma'_e(\phi)}{\Delta \rho g \phi}, \quad A(\phi) := \int_0^{\phi} a(s) ds, \quad (12)$$

we obtain the field equation

$$\frac{\partial \phi}{\partial t} + \frac{1}{S(x)} \frac{\partial}{\partial x} (Q_D(t)\phi + S(x)f_{\text{bk}}(\phi)) = \frac{1}{S(x)} \frac{\partial}{\partial x} \left(S(x)a(\phi) \frac{\partial \phi}{\partial x} \right), \quad (13)$$

which can also be written as

$$\frac{\partial(S(x)\phi)}{\partial t} + \frac{\partial}{\partial x} (Q_D(t)\phi + S(x)f_{\text{bk}}(\phi)) = \frac{\partial}{\partial x} \left(S(x) \frac{\partial A(\phi)}{\partial x} \right). \quad (14)$$

The numerical discretization (see Section 3) is based on the conservative form (14).

Eq. (8) corresponds to a special case of the mathematical model studied in this paper, namely that of $\sigma_e \equiv 0$. In fact, the case of batch sedimentation ($Q_D \equiv 0$) of ideal suspension in closed vessels, which corresponds to the equation

$$\frac{\partial \phi}{\partial t} + \frac{1}{S(x)} \frac{\partial}{\partial x} (S(x)f_{\text{bk}}(\phi)) = 0, \quad (15)$$

was thoroughly studied by Anestis (1981). Eq. (15), together with suitable boundary conditions, permits the construction of exact solutions by the method of characteristics. These solutions provide some qualitative insight into the structure of solutions of the parabolic-hyperbolic model equation (13). For this reason we have included in this paper a brief review of the method of characteristics applied to (15), see Section 4.

2.4. Initial and boundary conditions. We consider Eq. (13) for $0 < x < L$ and $0 < t \leq T$. At $t = 0$, an initial concentration distribution is given,

$$\phi(x, 0) = \phi_0(x), \quad 0 \leq x \leq L. \quad (16)$$

Being well aware that identifying the feed and discharge mechanisms is a strong simplification, we assume that at $x = L$ the vessel is fed with fresh suspension of concentration $\phi_F(t)$ at a volumetric rate $Q_F(t) \leq 0$. In terms of the coefficients of Eq. (13) or (14), this can be expressed as

$$\left(Q_D(t)\phi + S(L) \left[f_{bk}(\phi) - \frac{\partial A(\phi)}{\partial x} \right] \right) (L, t) = Q_F(t)\phi_F(t), \quad 0 \leq t \leq T. \quad (17)$$

At $x = 0$, we require that the solids flux ϕv_s reduces to its convective part $Q_D(t)\phi(0, t)$, and that $\phi(\cdot, t)$ is continuous across $x = 0$. This implies the boundary condition

$$\left(f_{bk}(\phi) - \frac{\partial A(\phi)}{\partial x} \right) (0, t) = 0, \quad 0 \leq t \leq T. \quad (18)$$

2.5. Properties of the mathematical model. Observe that $a(\phi)$, and thus the right-hand part of Equation (13), vanishes for $\phi \leq \phi_c$ or $\phi \geq \phi_{\max}$. Thus Eq. (13) is of first-order hyperbolic type for $\phi \leq \phi_c$, when it degenerates into (8), and of second-order parabolic type for $\phi_c < \phi < \phi_{\max}$. The hyperbolic and parabolic zones will also be referred to as *hindered settling* and *compression zones*, respectively. The location of the type-change interface $\phi = \phi_c$, that is the suspension-sediment interface, is not known beforehand. Since the equation degenerates from parabolic to hyperbolic type on the interval of (and not at isolated) solution values $[0, \phi_c]$, it is called *strongly degenerate*. Moreover, the diffusion coefficient $a(\phi)$ does not only vanish for $\phi \leq \phi_c$, but is under most circumstances even discontinuous at $\phi = \phi_c$, i.e. jumps at $\phi = \phi_c$ from zero to a positive value. This is due to the particular forms of effective solid stress function $\sigma_e(\phi)$ proposed in the literature.

These unusual features of Equation (13) and similar sedimentation-consolidation equations arising, for example, in the cases of batch centrifugation and (slightly simpler) batch and continuous sedimentation in vessels with $S \equiv \text{const.}$, gave rise to recent research in the mathematical and numerical analysis of certain strongly degenerate convection-diffusion equations, which lead to existence and uniqueness results as well as to appropriate numerical methods (see the discussion below). The most obvious difficulty in the treatment of Eq. (13) is caused by degeneration into a nonlinear first-order conservation law, since it is well known that solutions of such equations are discontinuous and have to be defined as weak solutions where an additional entropy condition has to be considered in order to single out the physically relevant solution.

The use of entropy conditions goes back to Kruřkov (1970) and Vol'pert and Hudjaev (1969). Existence, uniqueness and stability results for entropy solutions of strongly degenerate parabolic equations can be found in Bénilan and Touré (1995), Carrillo (1999), Chen and DiBenedetto (1999), Karlsen and Risebro (2000), Karlsen and Ohlberger (2001), Mascia et al. (2000), Rouvre and Gagneux (1999), Vol'pert and Hudjaev (1969), Vol'pert (2000) and Wu and Yin (1989). This literature treats both initial value and initial-boundary value problems. Mathematical theory for sedimentation-consolidation processes can be found in Bürger and Wendland (1998a,b), Bürger et al. (2000b) and Bürger and Karlsen (2001b).

Strictly speaking, the existing literature does not cover Eq. (14). However, by combining the methods by Carrillo (1999), Karlsen and Risebro (2000), and Karlsen and Ohlberger (2001) with those of Bürger et al. (2000b) and Bürger and Karlsen (2001b), one can prove existence and uniqueness of an entropy solution for Eq. (14) with initial and boundary conditions (16)–(18).

Regarding numerical methods, several different methods have been proposed and analyzed already in the literature. Let us mention the operator splitting methods by Evje and Karlsen (1999b)

and Holden et al. (2001), the finite difference schemes by Evje and Karlsen (1999a,2000), the finite volume schemes in Ohlberger (2001) and Eymard et al. (2000), the kinetic BGK schemes by Bouchut et al. (2000). For a partial overview of mathematical and numerical theory for degenerate parabolic equations based on “hyperbolic” techniques, see Espedal and Karlsen (2000). Numerical methods for sedimentation-consolidation processes can be found in Bürger et al. (2000c) and Bürger and Karlsen (2001a).

2.6. Steady states. As was shown elsewhere (Bustos et al., 1999), the analysis of steady states in a continuous thickener provides a method for thickener design. We show here that Eq. (13), together with its boundary conditions, provides a method for the construction of steady states. To this end, select $Q_D = \text{const.}$ and consider solutions of (13) which are stationary, i.e. independent of time. Such solutions satisfy the ordinary differential equation

$$Q_D \phi(x) + S(x) f_{\text{bk}}(\phi) = S(x) \frac{dA(\phi)}{dx} + C, \quad (19)$$

where C is a constant of integration. Taking into account the boundary condition (18) and assuming that $\phi_D > \phi_c$ is the desired solids discharge concentration, we obtain $C = Q_D \phi_D$. Inserting this into (19), we obtain the equation

$$Q_D (\phi(x) - \phi_D) + S(x) f_{\text{bk}}(\phi(x)) = S(x) \frac{dA(\phi)}{dx}. \quad (20)$$

For the compression zone, where ϕ varies between ϕ_c and ϕ_D , we have $a(\phi) \geq 0$ and $a(\phi) = 0$ at the critical height x_c , the sediment level, at which the critical concentration value ϕ_c is attained. For the corresponding concentration profile $\phi = \phi(x)$, we obtain the following initial-value problem (with respect to the independent variable x):

$$\frac{d\phi}{dx} = \frac{1}{a(\phi)} \left(\frac{Q_D}{S(x)} (\phi(x) - \phi_D) + f_{\text{bk}}(\phi(x)) \right), \quad x > 0, \quad (21a)$$

$$\phi(0) = \phi_D. \quad (21b)$$

Equation (21a) is integrated from $x = 0$ to x_c , that is until the critical concentration ϕ_c is attained. Assume that $0 < x_c < L$. The steady state concentration profile in the interval $(x_c, L]$ is determined by the condition that the solids volume feed flux F_F should equal the solids discharge flux, i.e., $F_F = Q_F \phi_F = Q_D \phi_D$. Then the algebraic equation

$$Q_D (\phi(x) - \phi_D) + S(x) f_{\text{bk}}(\phi(x)) = 0, \quad (22)$$

obtained from (20) for $\phi \leq \phi_c$, is consistent with the boundary condition (17). To determine the concentration in the interval $(x_c, L]$, Eq. (22) has to be solved for $\phi(x)$ for each $x \in (x_c, L]$. We assume here that the parameters Q_D and ϕ_D are chosen in such a way that Eq. (22) has a unique solution for all $x \in (x_c, H]$. Eq. (22) is equivalent to

$$Q_D \phi(x) + S(x) f_{\text{bk}}(\phi) = Q_D \phi_D = Q_F \phi_F, \quad (23)$$

which has a unique solution ϕ if the solids volume feed flux $Q_F \phi_F$ is sufficiently small.

Moreover, a steady state will be called admissible if the concentration increases downwards in the compression zone:

$$\frac{d\phi}{dx} \leq 0 \quad \text{for } 0 \leq x < x_c. \quad (24)$$

Consequently, we require that the right-hand part of (21a) is nonnegative for $0 \leq x < x_c$, or equivalently, that

$$Q_D (\phi(x) - \phi_D) + S(x) f_{\text{bk}}(\phi(x)) \leq 0 \quad \text{for } 0 \leq x \leq x_c. \quad (25)$$

Unlike the case $S \equiv \text{const.}$, where an easy geometric construction applies (see Bürger and Concha, 1998; Bürger et al., 1999; Bustos et al., 1999), it is not possible to state here precise a priori conditions under which (25) is satisfied. We will not discuss this problem in detail here but refer to Section 5.2 for a specific example.

2.7. Consistency with alternate formulations. The phenomenological theory of sedimentation-consolidation processes, which leads to the present model of continuous thickening, stipulates that a unique continuous function f_{bk} is given for the entire range of concentration values $[0, \phi_{\text{max}}]$, including the compression zone, where $\phi > \phi_c$. Semi-empirical formulae such as (9) are usually based on the assumption of absence of compressive stress, i.e. $\sigma_e \equiv 0$, and therefore their use seems to be appropriate in the hindered settling region (where $\phi < \phi_c$) only. This restriction is not necessary in order to obtain a well-posed mathematical model. However, a very instructive interpretation of the flux density function f_{bk} for $\phi > \phi_c$ is related to permeability.

Reverting to the linear momentum balances of the solid and the fluid, comparing the phenomenological approach with that of flow in porous media (Bürger et al., 2000a; Garrido et al., 2000) and assuming that the local permeability K of the sediment layer is a function of the porosity or, equivalently, of the solids concentration ϕ only, one can easily deduce that

$$f_{\text{bk}}(\phi) = -\frac{K(\phi)\Delta\rho g\phi^2}{\mu_f} \quad \text{for } \phi > \phi_c, \quad (26)$$

where μ_f is the dynamic viscosity of the pure fluid. Inserting (26) into (21a) and using (12), we obtain the ordinary differential equation

$$\frac{d\phi}{dx} = \frac{1}{\sigma_e'(\phi)} \left[\frac{Q_D\phi_D}{S(x)} \frac{\mu_f}{K(\phi)} \left(\frac{1}{\phi} - \frac{1}{\phi_D} \right) + \Delta\rho g\phi \right], \quad 0 < x < x_c \quad (27)$$

or

$$\frac{dx}{d\phi} = \sigma_e'(\phi) \left[\frac{Q_D\phi_D}{S(x)} \frac{\mu_f}{K(\phi)} \left(\frac{1}{\phi} - \frac{1}{\phi_D} \right) + \Delta\rho g\phi \right]^{-1}, \quad \phi_D > \phi > \phi_c \quad (28)$$

used in some of our previous papers (Resende et al. 1995, Freitas et al. 2000). The present paper is therefore an extension of our previous studies, in which only stationary solutions were considered, to the transient case.

For the relationship of the permeability and the effective stress to the local solids concentration, the following pair of model functions (usually attributed to Tiller and Leu, 1980) has frequently been utilized:

$$\phi = \phi_c(1 + \sigma_e/\sigma_0)^\beta, \quad K = K_0(1 + \sigma_e/\sigma_0)^{-\delta} \quad \text{for } \phi > \phi_c, \quad (29)$$

where $\beta > 0$ and $\delta > 0$ are parameters and K_0 and σ_0 denote the permeability and effective stress, respectively, at $\phi = \phi_c$. In view of (26), these equations can be converted into the following portion of the Kynch batch flux density function:

$$f_{\text{bk}}(\phi) = -\frac{K_0\Delta\rho g\phi_c^{\delta/\beta}}{\mu_f}\phi^{2-\delta/\beta} \quad \text{for } \phi > \phi_c, \quad (30)$$

and into the effective solid stress function

$$\sigma_e(\phi) = \begin{cases} 0 & \text{for } \phi \leq \phi_c, \\ \sigma_0[(\phi/\phi_c)^{1/\beta} - 1] & \text{for } \phi > \phi_c, \end{cases} \quad \text{i.e., } \sigma_e'(\phi) = \begin{cases} 0 & \text{for } \phi \leq \phi_c, \\ \sigma_0\phi_c^{-1/\beta}\beta^{-1}\phi^{1/\beta-1} & \text{for } \phi > \phi_c. \end{cases} \quad (31)$$

Note that the function σ_e' is discontinuous at $\phi = \phi_c$.

3. NUMERICAL METHOD FOR TRANSIENT SIMULATIONS

To simulate transient (non-stationary) batch and continuous sedimentation-consolidation processes in vessels with varying cross-sectional area, we solve the initial-boundary value problem of Eq. (14) together with the initial and boundary conditions (16)–(18) numerically using the generalized upwind method. This method is presented in detail by Bürger and Karlsen (2001), where the case of sedimentation in a cylindrical vessel is considered. Suitable modifications have been employed to simulate centrifugation (Bürger and Concha, 2001) and pressure filtration of flocculated suspensions (Bürger et al., 2001), so the presentation is very concise here.

On the computational domain $[0, L] \times [0, T]$ we introduce a standard rectangular grid having the mesh widths $\Delta x := L/J$ and $\Delta t := T/N$, where J and N are integers. We set $x_j := j\Delta x$,

$t_n := n\Delta t$ and $S_j := S(x_j)$ and let ϕ_j^n denote the approximate solution value at (x_j, t_n) . The computation starts by setting $\phi_j^0 := \phi_0(x_j)$ for $j = 0, \dots, J$.

Assume then that the solution values ϕ_j^n , $j = 0, \dots, J$ at the time level t_n have been calculated. The interior solution values ϕ_j^{n+1} , $j = 1, \dots, J-1$ are then given by the formula

$$\begin{aligned} \phi_j^{n+1} = \phi_j^n - \frac{1}{S_j} \left\{ \frac{\Delta t}{\Delta x} \left[Q_D(t_n)(\phi_{j+1}^n - \phi_j^n) + S_{j+1/2} f_{\text{bk}}^{\text{EO}}(\phi_j^n, \phi_{j+1}^n) - S_{j-1/2} f_{\text{bk}}^{\text{EO}}(\phi_j^n, \phi_{j-1}^n) \right] \right. \\ \left. - \frac{\Delta t}{\Delta x^2} \left[S_{j+1/2} (A(\phi_{j+1}^n) - A(\phi_j^n)) - S_{j-1/2} (A(\phi_j^n) - A(\phi_{j-1}^n)) \right] \right\}, \quad j = 1, \dots, J-1, \quad (32) \end{aligned}$$

where the numerical Kynch batch flux density function $f_{\text{bk}}^{\text{EO}}$ is given by

$$f_{\text{bk}}^{\text{EO}}(u, v) := f_{\text{bk}}(0) + \int_0^u \max\{f'_{\text{bk}}(s), 0\} ds + \int_0^v \min\{f'_{\text{bk}}(s), 0\} ds,$$

according to the Engquist-Osher numerical scheme (Engquist and Osher, 1980). To derive update formulae for the boundary solution values ϕ_0^n and ϕ_J^n , we approximate the boundary conditions (17) and (18) by the respective expressions

$$Q_D(t_n)\phi_{J+1}^n + S_{J+1/2} \left[f_{\text{bk}}^{\text{EO}}(\phi_J^n, \phi_{J+1}^n) - \frac{A(\phi_{J+1}^n) - A(\phi_J^n)}{\Delta x} \right] \approx Q_F(t_n)\phi_F(t_n) \equiv F_F(t_n), \quad (33)$$

$$f_{\text{bk}}^{\text{EO}}(\phi_{-1}^n, \phi_0^n) - \frac{A(\phi_0^n) - A(\phi_{-1}^n)}{\Delta x} \approx 0. \quad (34)$$

Inserting (33) and (34) into Eq. (32), we obtain the desired update formulae

$$\begin{aligned} \phi_J^{n+1} = \phi_J^n - \frac{1}{S_J} \left\{ \frac{\Delta t}{\Delta x} \left[Q_F(t_n)\phi_F(t_n) - Q_D(t_n)\phi_J^n - S_{J-1/2} f_{\text{bk}}^{\text{EO}}(\phi_J^n, \phi_{J-1}^n) \right] \right. \\ \left. + \frac{\Delta t}{\Delta x^2} S_{J-1/2} (A(\phi_J^n) - A(\phi_{J-1}^n)) \right\}, \\ \phi_0^{n+1} = \phi_0^n - \frac{1}{S_0} \left\{ \frac{\Delta t}{\Delta x} \left[Q_D(t_n)(\phi_1^n - \phi_0^n) + S_{1/2} f_{\text{bk}}^{\text{EO}}(\phi_0^n, \phi_1^n) \right] - \frac{\Delta t}{\Delta x^2} S_{1/2} (A(\phi_1^n) - A(\phi_0^n)) \right\}. \end{aligned}$$

To ensure convergence of the resulting scheme to the entropy (i.e. the physically relevant) solution of the initial-boundary value problem (14), (16)–(18), the following CFL stability criterion must be satisfied:

$$\frac{1}{S_{\min}} \left[\left(\max_{0 \leq t \leq T} |Q_D(t)| + S_{\max} \max_{0 \leq \phi \leq \phi_{\max}} |f'_{\text{bk}}(\phi)| \right) \frac{\Delta t}{\Delta x} + 2 \max_{0 \leq \phi \leq \phi_{\max}} a(\phi) \frac{\Delta t}{\Delta x^2} \right] \leq 1, \quad (35)$$

where $S_{\min} := \min_{0 \leq x \leq H} S(x)$ and $S_{\max} := \max_{0 \leq x \leq H} S(x)$. To ensure (35) in the numerical examples, Δx is selected freely and Δt is determined by

$$\Delta t = \frac{0.98 S_{\min} \Delta x}{\max |Q_D(t)| + S_{\max} \max |f'_{\text{bk}}(\phi)| + \frac{2 \max a(\phi)}{\Delta x}}.$$

4. BATCH SEDIMENTATION OF IDEAL SUSPENSIONS IN CLOSED CONICAL VESSELS

To appropriately put the mathematical model into the perspective of existing results, most notably the kinematic wave theory developed in Anestis' thesis (Anestis, 1981), we briefly recall the basic ideas of the method of characteristics as applied to Eq. (15), with an emphasis on the differences to the constant cross-section case. Similar considerations apply to models of batch centrifugation of ideal suspensions (Anestis and Schneider, 1983; Bürger and Concha, 2001).

To outline the main ideas, we rewrite Eq. (15) as

$$\frac{\partial \phi}{\partial t} + \frac{\partial f_{\text{bk}}(\phi)}{\partial x} = - \frac{S'(x) f_{\text{bk}}(\phi)}{S(x)}. \quad (36)$$

It is now convenient to regard

$$f(x, t) := -f_{\text{bk}}(\phi(x, t)) \quad (37)$$

as dependent variable. We assume that there exists a function g such that $\phi = g(f)$. Then (36) can be rewritten as

$$g'(f) \frac{\partial f}{\partial t} - \frac{\partial f}{\partial x} = \frac{S'(x)f}{S(x)}. \quad (38)$$

We now assume that S is a monotonous function of x , such that there exists an inverse function h with $x = h(S(x))$. Moreover, we define the function p by $p(S) := S'(h(S))$.

The application of the method of characteristics to Eq. (38) yields that the solution $f = f(x, t)$ of Eq. (38) has the representation

$$x = q(f, \xi) := h(f_0 S(\xi)/f), \quad t = \tau(f, \xi) := f_0 S(\xi) \int_{f_0}^f \frac{g'(y)}{y^2 p(f_0 S(\xi)/y)} dy, \quad (39)$$

where the parameter ξ is constant along characteristics and has been selected in such a way that $\xi = x$ for $t = 0$. Note that it is the parameter ξ and not the solution ϕ which is constant along characteristics, and thus characteristics are in general not iso-concentration lines, except in the cylindrical case $S = \text{const.}$

Eq. (39) holds wherever the solution is continuous. However, intersections of characteristics cause solutions of (36) to be discontinuous in general. The propagation speed σ of a discontinuity Σ at a point $(x, t) \in \Sigma$ in the (x, t) -plane, which separates two concentration values ϕ^- and ϕ^+ , is given by the Rankine-Hugoniot condition

$$\sigma(\phi^+, \phi^-) = \left. \frac{dx}{dt} \right|_{\Sigma} = \frac{f_{\text{bk}}(\phi^+) - f_{\text{bk}}(\phi^-)}{\phi^+ - \phi^-}. \quad (40)$$

In terms of the independent variable f , Eq. (40) can be rewritten as

$$\sigma(\phi^+, \phi^-) = \tilde{\sigma}(f^+, f^-) = -\frac{f^+ - f^-}{g(f^+) - g(f^-)}. \quad (41)$$

Using the total differentials

$$dx = \frac{\partial q}{\partial f} df + \frac{\partial q}{\partial \xi} d\xi, \quad dt = \frac{\partial \tau}{\partial f} df + \frac{\partial \tau}{\partial \xi} d\xi \quad (42)$$

we obtain

$$\left. \frac{dx}{dt} \right|_{\Sigma} = -\frac{\frac{\partial q}{\partial f} df + \frac{\partial q}{\partial \xi} d\xi}{\frac{\partial \tau}{\partial f} df + \frac{\partial \tau}{\partial \xi} d\xi} = -\frac{f^+ - f^-}{g(f^+) - g(f^-)}. \quad (43)$$

Rearranging the right equation in (43) we obtain the following ordinary differential equation:

$$\frac{d\xi}{df} = \frac{\frac{\partial q}{\partial f}(g(f^+) - g(f^-)) - \frac{\partial \tau}{\partial f}(f^+ - f^-)}{\frac{\partial \tau}{\partial \xi}(f^+ - f^-) - \frac{\partial q}{\partial \xi}(g(f^+) - g(f^-))}. \quad (44)$$

The solution $\xi = \Xi(f)$ of (44) represents the discontinuity Σ in the (ξ, f) -plane, that is the characteristic plane. We can transform the solution $\xi = \Xi(f)$ from the characteristic plane into the physical (x, t) -plane by determining for each point (ξ, f) of the characteristic plane its physical coordinates $x = q(\xi, f)$ and $t = \tau(\xi, f)$ by making use of (39). The curves $\xi = \text{const.}$ and $f = \text{const.}$ in the physical (x, t) -plane are given by (39) if one coordinate is kept fixed and the other is considered as a parameter.

The method of characteristics permits in principle the construction of exact discontinuous solutions to Eq. (15) by analytical means. However, curved shock trajectories occur, which can be computed only by integrating numerically an ordinary differential equation. We refer to Chapter 3 of Anestis (1981) for detailed constructions of such weak solutions by the method of characteristics but present here solutions of Eq. (15) obtained by the numerical method described in Section 3, and setting $\sigma_e \equiv 0$.

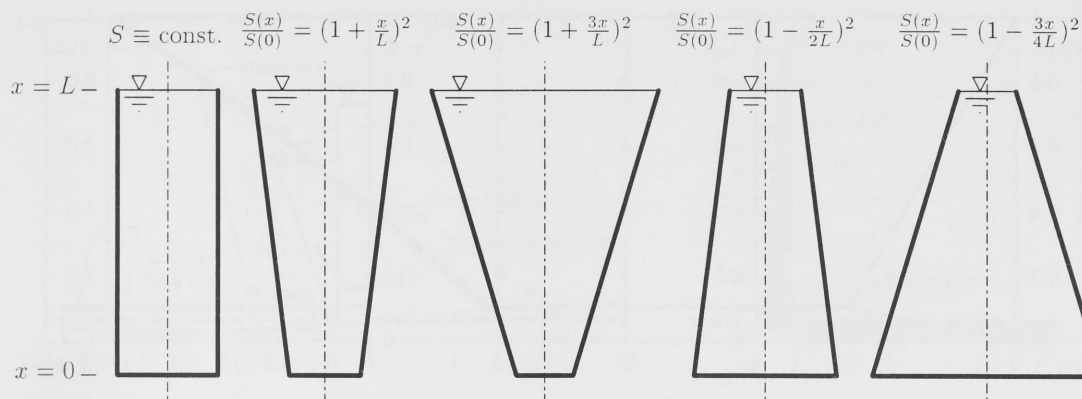


FIGURE 1. Examples of the vessels (here with circular cross-sectional area for every height) considered for batch sedimentation of ideal (L is an arbitrary height) or flocculated suspensions ($L = 1$ m).

We choose the function f_{bk} given by (9) with the parameters $\phi_{\max} = 1$, according to the well-known Richardson and Zaki equation (Richardson and Zaki, 1954), and $n = 5$ as in Anestis (1981), Anestis and Schneider (1983) and Bürger and Concha (2001) in order to make results comparable. The solution is independent of the constant u_{∞} if we consider a vessel of height L and refer t to the time $T = L/u_{\infty}$, which is the time a single particle needs to travel through the vessel.

We consider five different cylindrical or conical vessels, see Figure 1. As in the centrifugation examples discussed in Section 4.2 of Bürger and Concha (2001), the initial concentration $\phi_0 = 0.07$ is chosen. This value corresponds to a Mode of Sedimentation MS-1 (Bustos et al., 1999; Bürger and Tory, 2000) in a closed settling column with $S \equiv \text{const}$. Figure 2(a) shows this solution, which consists at first of one descending discontinuity (or kinematic shock) separating the suspension at initial concentration from the supernatant clear liquid and one rising discontinuity separating the suspension from the sediment, where $\phi = \phi_{\max}$. At the so-called critical time t_c these shocks meet and form a third stationary shock separating the sediment from the clear liquid. The corresponding concentration profiles, which are simply structured, are shown in Figure 2(b).

In Figure 2(c) and (d), we consider the same initial concentration, vessel height and flux density function, but assume now that the vessel is of conical shape, with the top cross-sectional area being four times as large as that of the bottom. We observe that the propagation speed of the downwards propagating supernatant-suspension interface continuously decreases (in absolute value), producing a discontinuity curve of convex shape. Below that interface the concentration no longer remains constant, but increases, and the sediment is no longer separated from the suspension by a simple concentration discontinuity, as in an MS-1, but by a composition of waves emerging from the origin. All these features are even more pronounced in Figure 2(e) and (f), where the ratio between top and bottom cross-sectional area is 16. Observe in Fig. 2(e) that some of the numerically calculated iso-concentration lines, e.g. that for $\phi = 0.4$, are clearly curved, and that the concentration profiles plotted in Fig. 2(f) indicate that this is not a case of a true curved shock. Curved iso-concentration lines are, however, impossible in the cylindrical case, in which iso-concentration lines are always straight characteristics.

Figure 3 presents calculations for the same vessels turned upside-down, i.e. the cross-sectional area increases by factors four (Fig. 3(a,b)) and 16 (Fig. 3(c,d)) downwards. We observe effects that are contrary to those of Fig. 2: the propagation velocity of the suspension-supernatant interface increases (in absolute value) downwards and the concentration of the bulk suspension decreases. Moreover the suspension is separated from the sediment by a discontinuity.

Figures 2 and 3 illustrate that the structures of solutions to the problem of sedimentation of an initially homogeneous ideal suspension in conical vessels are more complicated than in the cylindrical case, and that the downwards increase (decrease) of diameter accelerates (retards) the

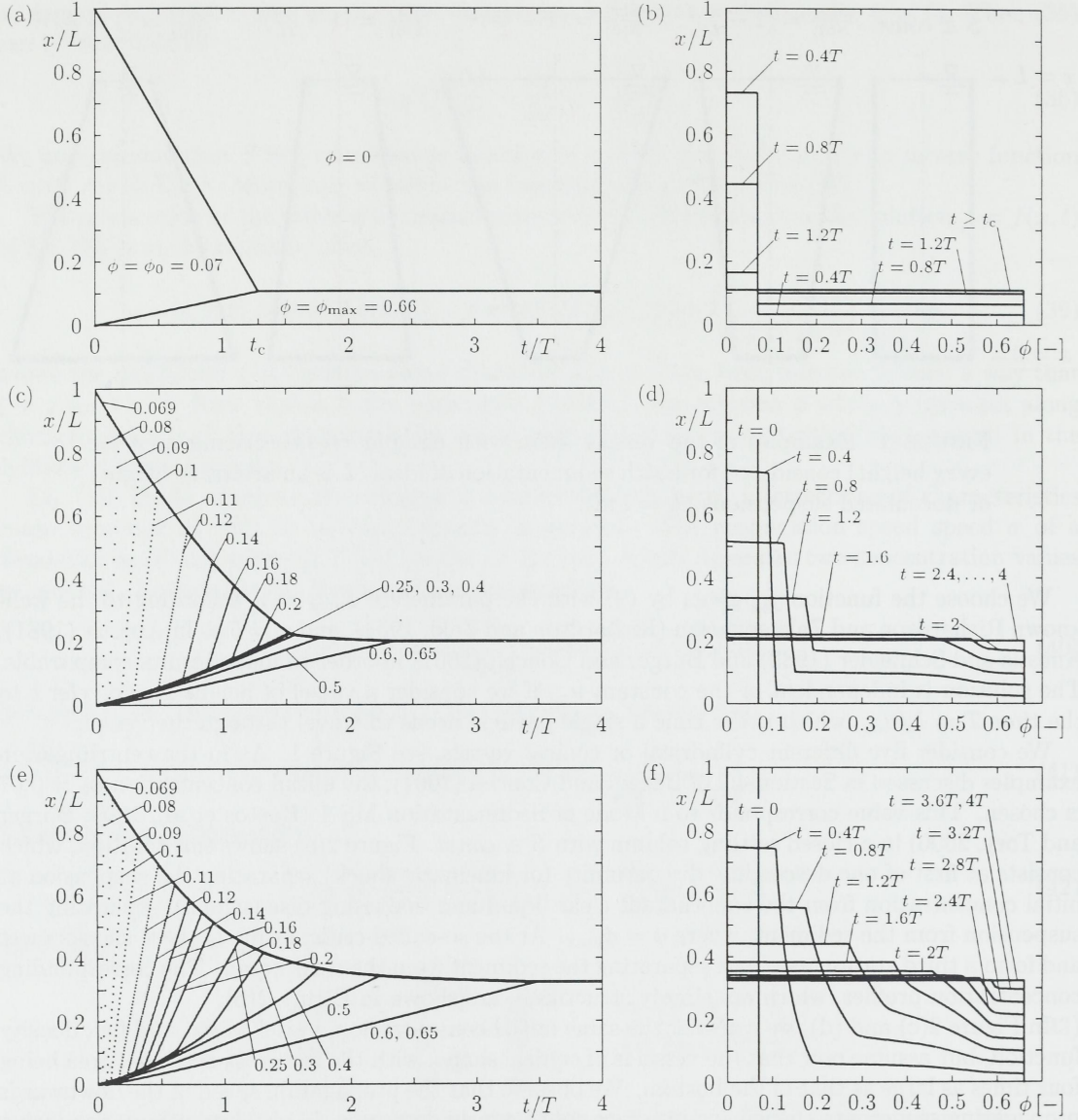


FIGURE 2. Sedimentation of an ideal suspension in conical vessels with (a,b) $S \equiv \text{const}$, (c,d) $S(x)/S(0) = (1+x/L)^2$ and (e,f) $S(x)/S(0) = (1+3x/L)^2$.

completion of the sedimentation process observed in a cylindrical vessel of the same height. These properties were already observed by Anestis (1981), who determined exact solutions to the same problem by the methods of characteristics but considered the simpler quadratic Kynch batch flux density function (9) with $\phi_{\max} = 1$ and $n = 1$. The different final sediment heights in Figures 2 and 3 are, of course, a trivial consequence of the vessel geometry.

5. NUMERICAL EXAMPLES: BATCH AND CONTINUOUS SEDIMENTATION OF FLOCCULENT SUSPENSIONS

5.1. Application to a hypothetical flocculated suspension. We consider a flocculent suspension with $\Delta\rho = 1660 \text{ kg/m}^3$ whose model functions f_{bk} and σ_e are given by Eq. (9) with the parameters $\phi_{\max} = 1$, $C = 5$ (as before) and $u_\infty = -1.0 \times 10^{-4} \text{ m/s}$ and Eq. (31) with $\phi_c = 0.1$, $\sigma_0 = 5.7 \text{ Pa}$ and $\beta = 1/9$. The parameters of the effective stress function correspond to a slurry

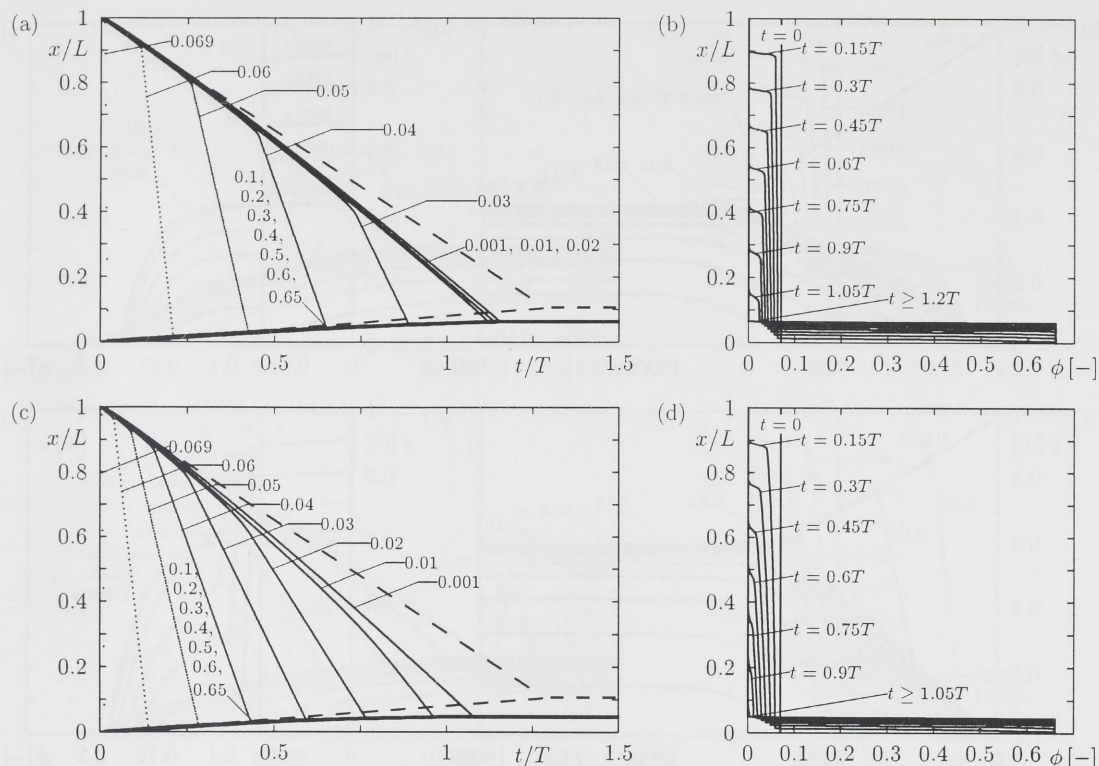


FIGURE 3. Sedimentation of an ideal suspension in conical vessels with (a,b) $S(x)/S(0) = (1 - 0.5x/L)^2$ and (c,d) $S(x)/S(0) = (1 - 0.75x/L)^2$. The dashed lines correspond to the kinematic shocks of Figure 2(a).

used by Damasceno et al. (1992). The same constitutive functions f_{bk} and σ_e are also used for centrifugation sample calculations by Bürger and Concha (2001), such that results may be compared.

5.1.1. Simulation of batch settling. We consider the settling of an initially homogeneous suspension of the initial concentration $\phi_0 = 0.07$ in five different vessels of height $L = 1$ m. Note that due to the dynamic effects, solutions are no longer dimensionless. Figure 4 shows the settling plots (left column) and sequences of concentration profiles (right column) for a cylindrical tank (a,b) and conical vessels with $S(1)/S(0) = 4$ (c,d) and $S(1)/S(0) = 16$ (e,f). Observe that the iso-concentration lines become horizontal, and thus the consolidation process terminates earlier, as the opening angle of the cone widens. Conversely, the consolidation process terminates later in conical vessels with downward-facing walls, as seen in the simulations of Figure 5, where $S(1)/S(0) = 1/4$ (a,b) and $S(1)/S(0) = 1/16$ (c,d). Note that the shape of the final concentration stationary concentration profile is the same (up to vertical shifts) for all five cases of Figures 4 and 5, independent of their shape. This is an easy consequence of the ordinary differential equation for steady state profiles (21a), in which the term containing the area function $S(x)$ disappears if we set $Q_D = 0$ corresponding to batch settling. This observation was also stated by Freitas et al. (2000).

5.1.2. Analysis of steady states. Consider a flocculated suspension defined by the model functions stated at the beginning of this section. The feed concentration is assumed to satisfy $\phi_F \geq 0.05$. Assume that the desired discharge concentration is $\phi_D = 0.235$ and that the solids volume feed rate is $F_F = Q_F \phi_F = -0.0000235$ m/s. We are now interested in the *height* and the *volume* of a cylindrical or conical thickener that is able to handle the thickening problem in conventional operation.

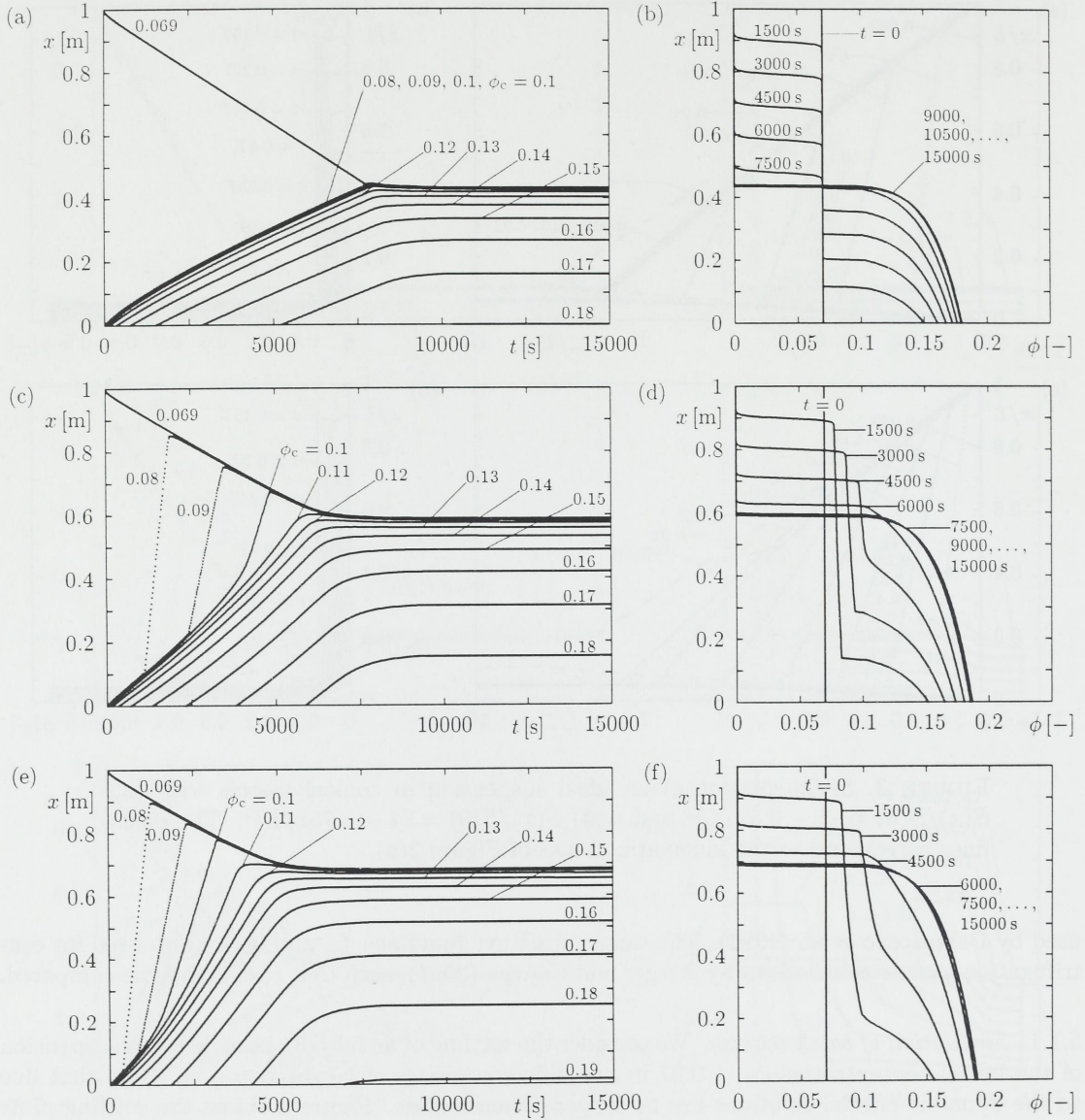


FIGURE 4. Simulation of sedimentation of a flocculated suspension in conical vessels with $L = 1$ m and (a,b) $S \equiv \text{const}$, (c,d) $S(x)/S(0) = (1 + x/L)^2$ and (e,f) $S(x)/S(0) = (1 + 3x/L)^2$.

The data of the problem are chosen such that the volume discharge rate of concentrated sediment is $Q_D = -0.0001 \text{ m}^3/\text{s}$. We now consider three different vessels and attempt to construct steady states for various discharge concentrations ϕ_D .

- (a) Cylindrical thickener of cross-sectional area $S \equiv 1 \text{ m}^2$. For cylindrical vessels, the flux function relevant for the conventional steady state analysis (Bürger et al. 1999, Bustos et al. 1999) is

$$f(\phi) = q\phi + f_{bk}(\phi); \quad q = Q_D/S.$$

An admissible stationary concentration profile can according to condition (25) (with $S \equiv \text{const.}$) exist only if

$$f(\phi) \leq q\phi_D \quad \text{for } \phi_c \leq \phi \leq \phi_D. \quad (45)$$

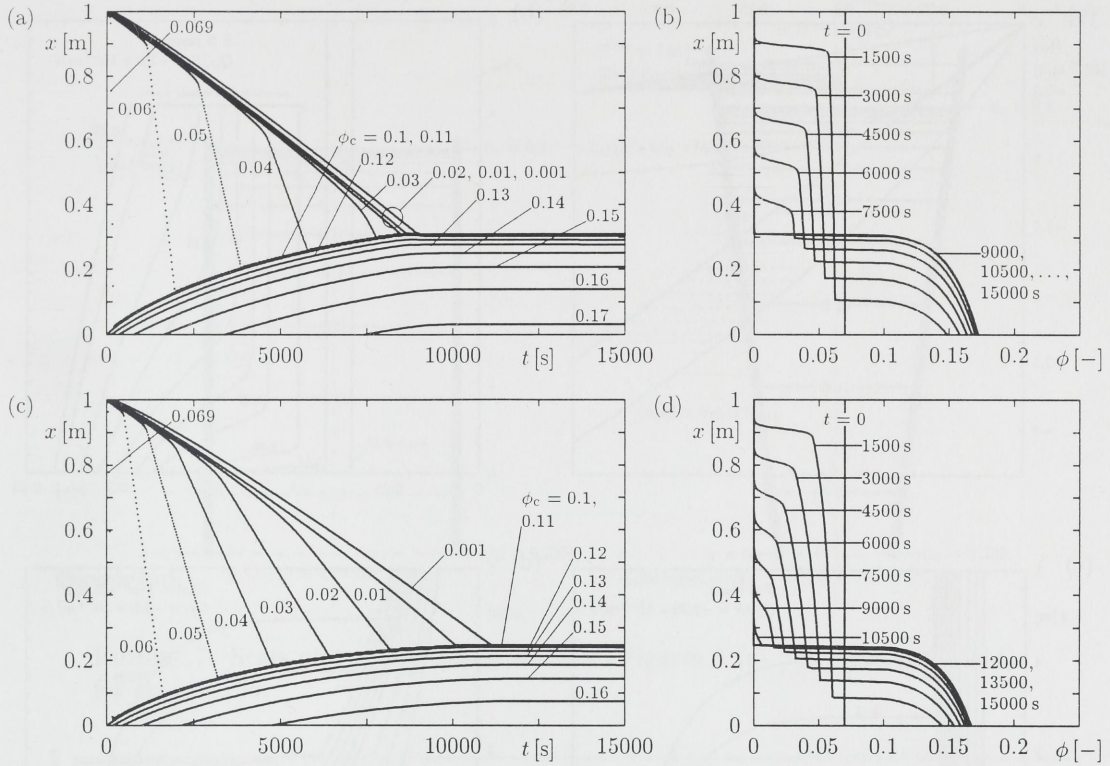


FIGURE 5. Sedimentation of a flocculated suspension in conical vessels with (a,b) $S(x)/S(0) = (1 - 0.5x/L)^2$ and (c,d) $S(x)/S(0) = (1 - 0.75x/L)^2$.

The flux plot in Figure 6 (a) with $q = q^1 = Q_D/(1 \text{ m}^2)$ reveals that condition (45) is satisfied only for $\phi_D = 0.12$ or $\phi_D = 0.14$, but not for the selected values $\phi_D = 0.16$ to 0.235 . Figure 6 (b) shows the two admissible steady states and the attempts to calculate steady states in the inadmissible cases ($\phi_D = 0.16, \dots, 0.235$), which results in vertical asymptotic concentration lines corresponding to the intersections of the dashed lines in Figure 6 (a) with the flux plot. Obviously this cylindrical thickener can not handle the thickening problem. (It could if we chose $\phi_D = 0.12$ or 0.14 .)

- (b) We now successively increase the area S or reduce (in absolute value) $q = Q_D/S$. This will increase the range of values of ϕ_D that lead to admissible steady states. Taking into account that the feed suspension should be *diluted* to the steady state concentration valid above the sediment level, we seek the largest (in absolute value) q such that $\phi_D = 0.235$ produces an admissible steady state with $\phi|_{x>x_c} \leq 0.05$. This occurs for $q = q^2 = -2.09 \times 10^{-5} \text{ m/s}$. The flux plot in Figure 6 (a) confirms that the steady states for all values of ϕ_D considered are admissible. Figure 6 (c) shows the corresponding concentration profiles. We can see that the required *height* of the corresponding thickener (not taking into account safety factors) is $x_c^{\text{cyl}} = 4.1 \text{ m}$. The *area* necessary to treat the thickening problem is given by

$$S = \frac{Q_D}{q} = \frac{-0.0001 \text{ m}^3/\text{s}}{-0.0000209 \text{ m/s}} = 4.785 \text{ m}^2.$$

Consequently, the thickener *volume* required is

$$V^{\text{cyl}} = x_c^{\text{cyl}} \cdot S = 19.617 \text{ m}^3.$$

- (c) Conical thickener with $S(x) = 1 + Cx^2$ [m^2], $C = 0.16$, i.e. $S(0) = 1 \text{ m}^2$, $S(5 \text{ m}) = 5 \text{ m}^2$. Figure 6 (d) shows the steady state concentration profiles for this vessel and the discussed values of ϕ_D . Obviously, these profiles are all admissible, and the concentrations in the

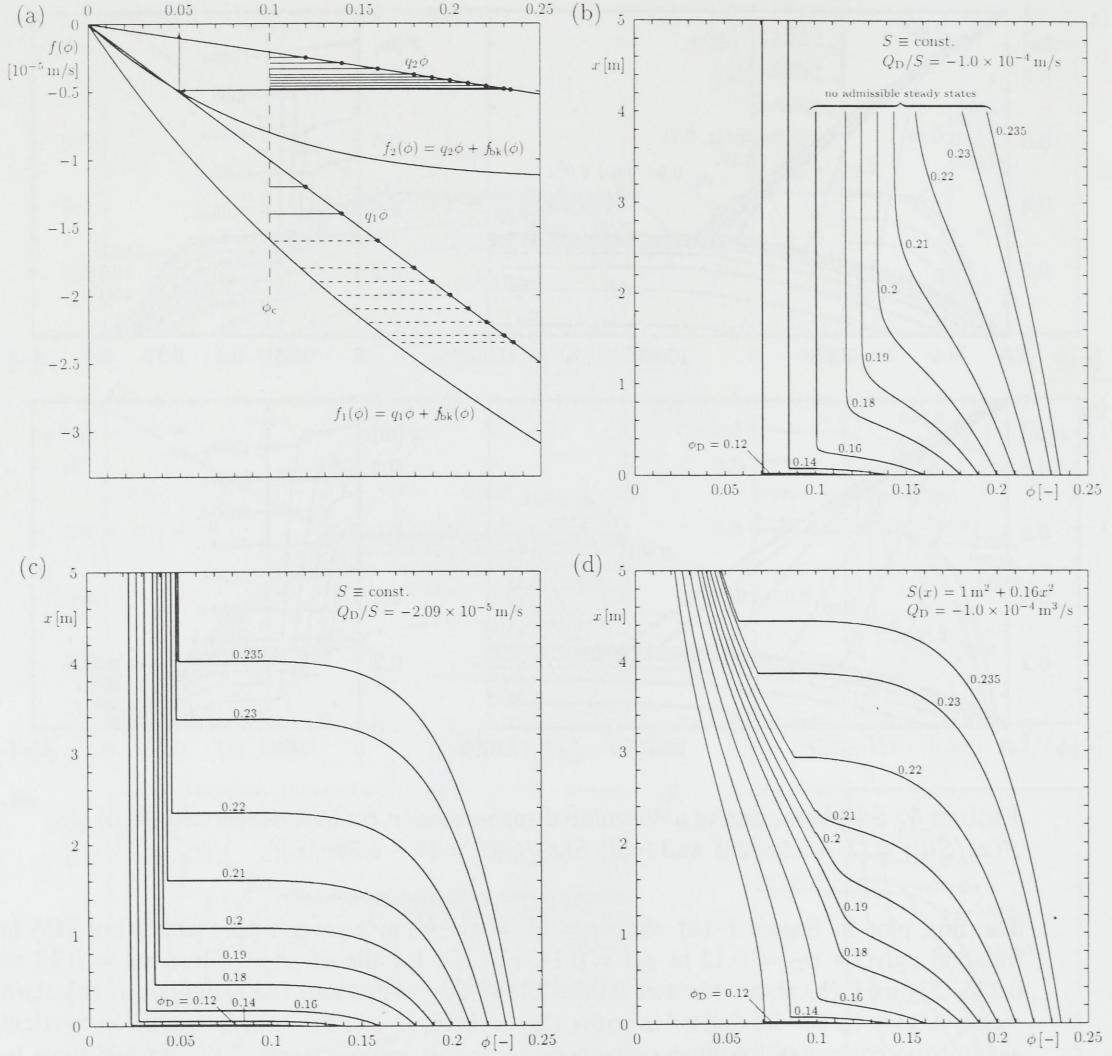


FIGURE 6. Steady states in cylindrical and conical vessels. (a) Flux plot for a cylindrical vessel at the bulk flow velocities $q_1 = Q_D^1/S = -1.0 \times 10^{-4} \text{ m/s}$ and $q_2 = Q_D^2/S = -2.09 \times 10^{-5} \text{ m/s}$. The horizontal solid and dashed lines correspond to admissible and inadmissible steady states, respectively. (b,c) Steady states in a cylindrical vessel at (b) $Q_D/S = q_1$ and (c) $Q_D/S = q_2$. (d) Steady states in a conical vessel.

hindered settling zones are not constant, as a consequence of Eq. (23). We performed calculations with different shape factors C and chose C so small that the steady state concentration at height $x = 5 \text{ m}$ does not exceed 0.05, such that the required dilution of the feed suspension is possible.

Note that due to the varying concentrations in the hindered settling zone, the minimum height H^{con} of this conical vessel is not identical to the sediment height and larger than that of the cylindrical; we may take here $H^{\text{con}} = 5 \text{ m}$. However, the volume of this conical vessel is given by

$$V^{\text{con}} = \frac{H^{\text{con}}}{3} \left(S(0) + \sqrt{S(0)S(H^{\text{con}})} + S(H^{\text{con}}) \right) = \frac{5}{3}(1 + \sqrt{5} + 5) \text{ m}^3 = 13.727 \text{ m}^3.$$

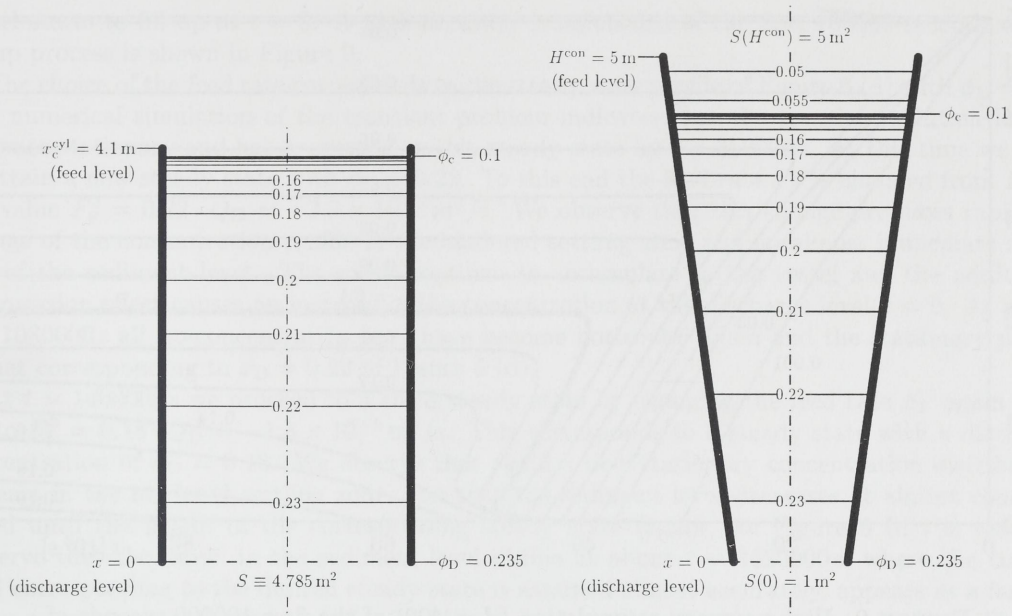


FIGURE 7. Scale plot of the steady states of Figures 6 (c) (left) and (d) (right) for $\phi_D = 0.235$.

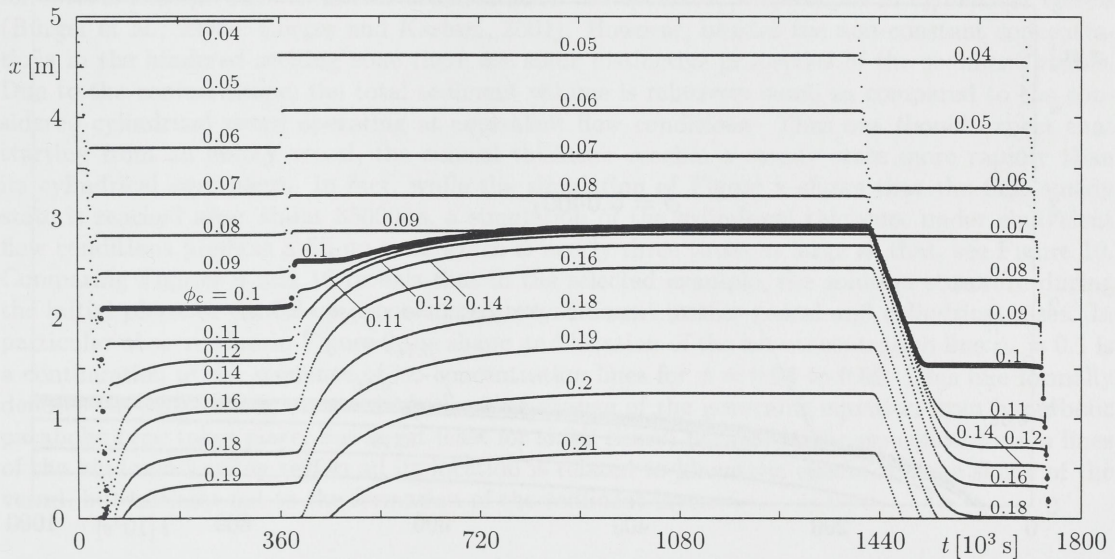


FIGURE 8. Simulation of continuous thickening in a conical thickener (Case (c) in Sect. 5.1.2): transition between steady states. The iso-concentration lines correspond to the annotated values. The spatial discretization parameter is $J = 200$.

We conclude that the volume of a conical thickener needed to handle the thickening problem is 30% smaller than the volume of the smallest cylindrical vessel designed for the same task. Figure 7 shows scale diagrams of the cylindrical and the conical tank operating at steady state.

5.1.3. *Simulation of the transient behaviour of a conical continuous thickener.* We continue to discuss the thickening problem of Sect. 5.1.2 and employ the numerical algorithm described in

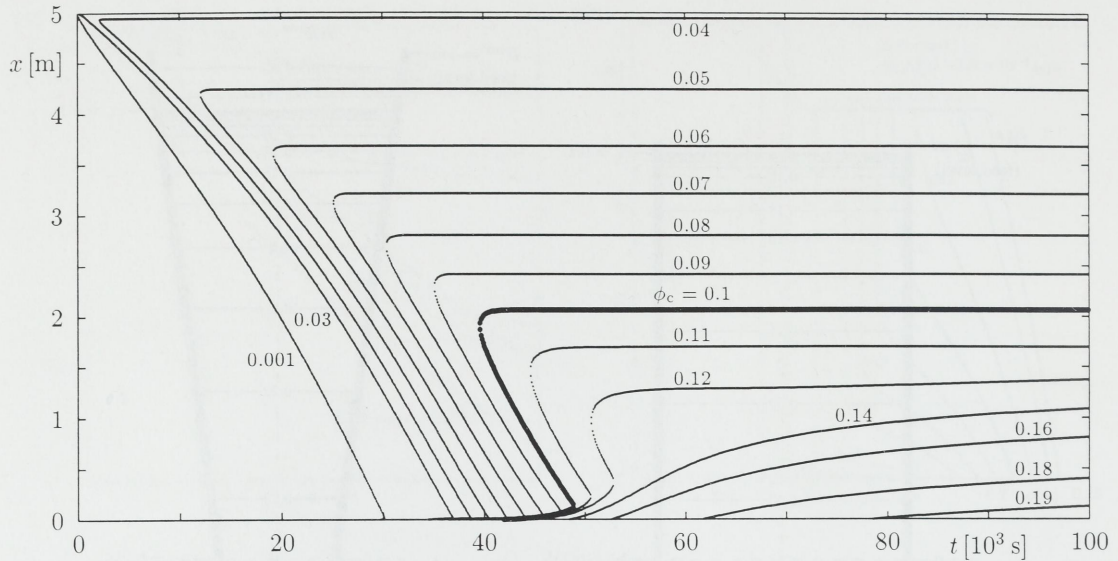


FIGURE 9. High-accuracy resimulation ($J = 400$) of the first 100000 seconds of the fill-up of the conical thickener shown in Figure 8. The iso-concentration lines correspond to the annotated values.

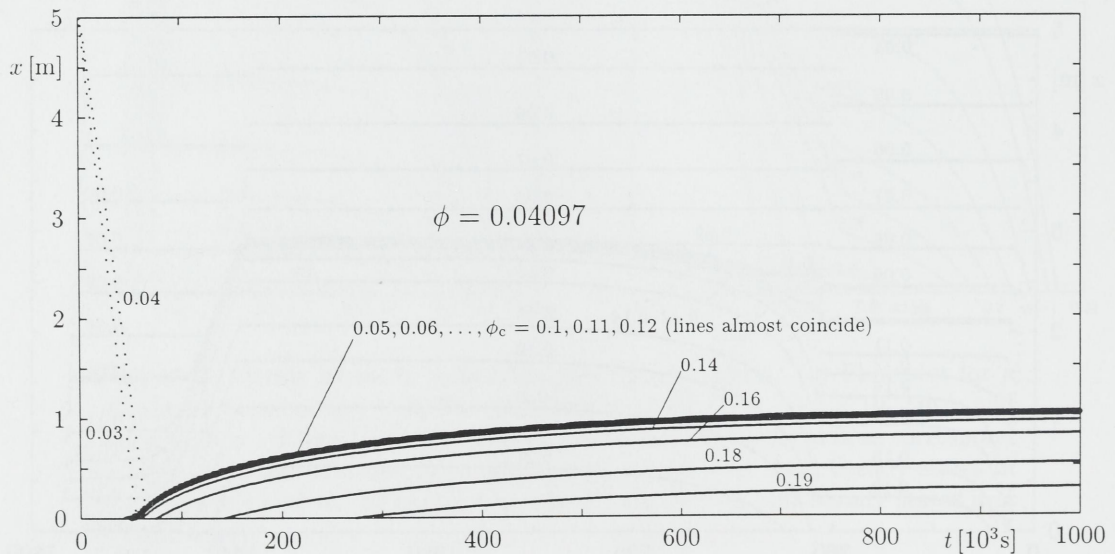


FIGURE 10. Simulation of the fill-up of the cylindrical continuous thickener (Case (b) in Sect. 5.1.2) at $q = -2.09 \times 10^{-5}$ m/s and $f_F = q \cdot 0.2 = -4.18 \times 10^{-6}$ m/s. The discretization parameter is $J = 200$.

Sect. 3 to simulate the processes of filling up the conical vessel of Case (c), transitions between steady states and emptying it. To this end, we assume that the conical thickener is initially full of water, i.e. $\phi_0 \equiv 0$, and that during the whole simulated time interval of 1.8×10^6 s it is discharged at the constant volume rate of $Q_D = -0.0001$ m³/s. Thus the only control actions taken are changes of the solids volume feed rate $F_F = Q_F \phi_F$.

At $t = 0$ we start filling up the vessel by setting $F_F = F_F^1 = 0.20 \cdot Q_D = -2.0 \times 10^{-5}$ m³/s. As can be seen in the settling plot showing the numerical solution of the problem (Figure 8), the

vessel starts to fill up at $t = 0$. A high-accuracy resimulation of the first 100000 seconds of the fill-up process is shown in Figure 9.

The choice of the feed rate corresponds to the steady state profile of Figure 6 (d) with $\phi_D = 0.2$. The numerical simulation of the transient problem indicates that the transient solution indeed becomes stationary and has converged to this steady state by $t = 350000$ s. At this time we wish to attain a new steady state with $\phi_D = 0.22$. To this end the feed rate F_F is changed from F_F^1 to the value $F_F^2 = 0.22 \cdot Q_D = -2.2 \times 10^{-5} \text{ m}^3/\text{s}$. We observe that this change produces rapidly a change of the concentration profile in the hindered settling zone and an almost immediate slight rise of the sediment level. The solids continue to accumulate in the vessel and the additional compression effect causes an increase of the concentration at the discharge level $x = 0$. At about $t = 1080000$ s all iso-concentration lines have become horizontal again and the stationary profile is that corresponding to $\phi_D = 0.22$ of Figure 6 (d).

At $t = 1400000$ s we proceed to a third steady state by changing the feed rate F_F again from F_F^2 to $F_F^3 = 0.18 \cdot Q_D = -1.8 \times 10^{-5} \text{ m}^3/\text{s}$. This corresponds to a steady state with a discharge concentration of $\phi_D = 0.18$. We observe that again a new stationary concentration distribution appears in the hindered settling zone, and that the sediment level decreases at almost constant speed until the height of the corresponding steady state (again, see Figure 6 (d)) is reached. Observe that the 'kink' in the sediment level visible at about $t = 1520000$ s, where the correct level corresponding to the desired steady state is attained almost accurately, appears as a feature of the approximate numerical solution and is not produced by a particular control action. Finally, at $t = 1700000$ s the simulated feed mechanism is turned off by changing F_F from F_F^3 to zero. Given that the discharge flow persists, the conical thickener empties rapidly.

The simulated evolution of the sediment composition is at a first look similar to that calculated for several examples of continuous sedimentation of flocculated suspensions in cylindrical vessels (Bürger et al., 2000c; Bürger and Karlsen, 2001). However, besides the non-constant concentrations in the hindered settling zone there are some distinctive properties of the sediment visible. Due to the conical shape, the total sediment volume is relatively small as compared to the considered cylindrical vessel operating at equivalent flow conditions. Thus one should expect that starting from an empty vessel, the conical thickener reaches a steady state more rapidly than its cylindrical equivalent. In fact, while the simulation of Figure 8 shows that the first steady state is reached after about 350000 s, a simulation of the cylindrical thickener under equivalent flow conditions predicts a fill-up time which is nearly three times as large as that, see Figure 10. Comparing Figures 9 and 10 reveals that in the selected example, the solution structure during the initial phase of the fill-up process is entirely different in the conical and cylindrical cases. In particular observe that in Figure 9 the shape and location of the iso-concentration line $\phi_c = 0.1$ is a continuation of the sequence of iso-concentration lines for $\phi = 0.04$ to 0.09. This line formally denotes the sediment level, at which the type change of the governing equation from hyperbolic parabolic type takes place, but is (at least for small times) parallel to the iso-concentration lines of the hindered settling region and its location is related to kinematic effects and the shape of the vessel, but initially not to the formation of the sediment layer.

5.2. Application to experimental results.

5.2.1. *Constitutive equations.* In this paper we consider experimental results of batch and continuous sedimentation of an aqueous calcium carbonate suspension of density difference $\Delta\rho = 1652 \text{ kg/m}^3$. The constitutive equations for the compression zone were chosen according to the approach by Tiller and Leu (1980), Eq. (29), with the parameters $\phi_c = 0.14$, $\sigma_0 = 11.0 \text{ Pa}$, $\beta = 0.12$, $\delta = 0.5196$ and $K_0 = 2.4 \times 10^{-13} \text{ m}^2$ (Damasceno, 1992; Freitas et al. 2000). Assuming the parameter values $g = 9.81 \text{ m/s}^2$ and $\mu_f = 0.001 \text{ Pa} \cdot \text{s}$, we obtain from these values the effective solid stress function

$$\sigma_e(\phi) = \begin{cases} 0 & \text{for } \phi \leq \phi_c = 0.14, \\ 11 [(\phi/\phi_c)^{8.33} - 1] \text{ Pa} & \text{for } \phi > \phi_c. \end{cases} \quad (46)$$

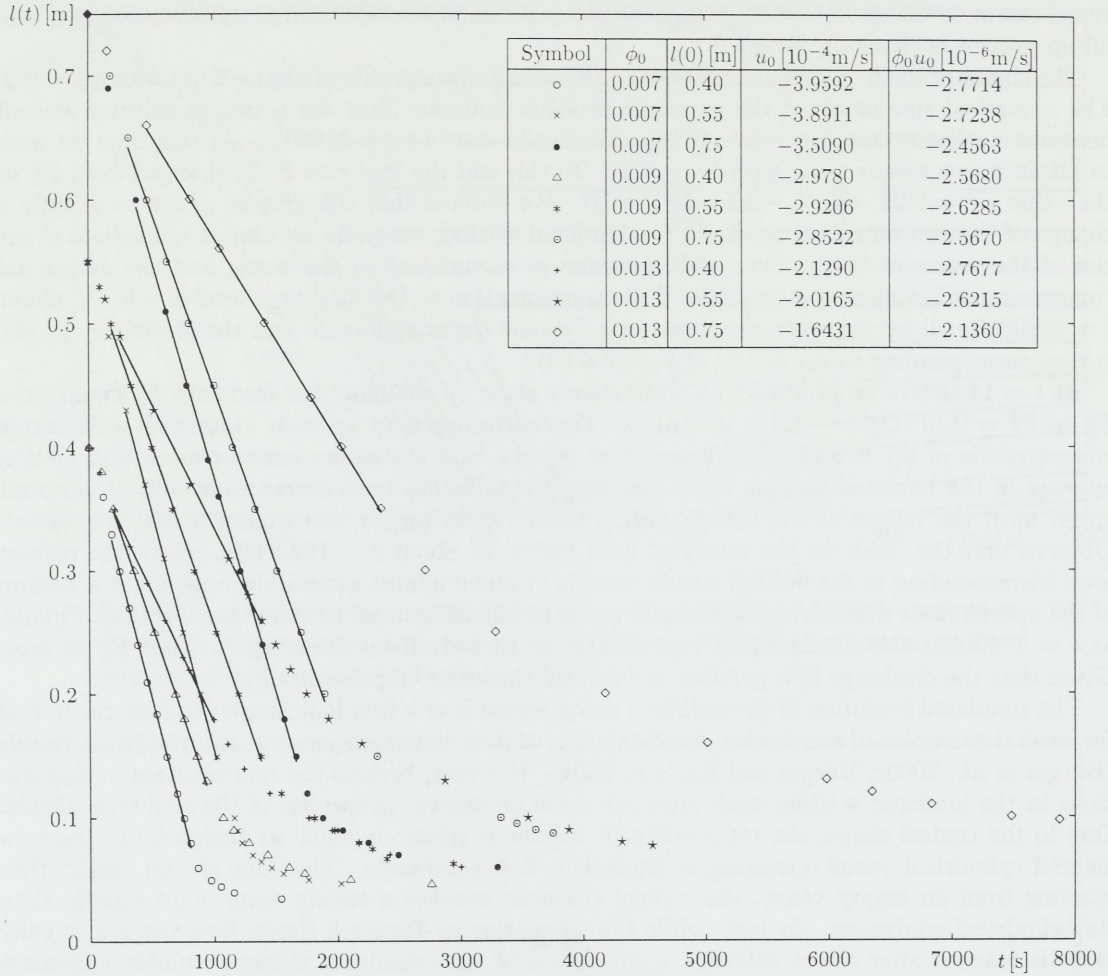


FIGURE 11. Supernate-suspension interfaces $l(t)$ measured for batch sedimentation of aqueous calcium carbonate suspensions (Damasceno, 1992). The solid straight lines with slopes u_0 approximate the parts of the data showing nearly constant settling velocity.

and, using Eq. (30), the following portion of the Kynch batch flux density function:

$$f_{\text{bk}}(\phi) = -7.8095 \times 10^{-10} \phi^{-2.33} \text{ m/s} \quad \text{for } \phi > 0.14. \quad (47)$$

Note that the information of Eqns. (46) and (47) is already sufficient for the determination of the sediment profiles of steady states. To find a reasonable choice for the hindered settling part of f_{bk} , we utilize data obtained from batch settling experiments with the same calcium carbonate suspension at the initial concentrations $\phi_0 = 0.007$, 0.009 and 0.013 in vessels of heights 0.40 m, 0.55 m and 0.75 m and constant cross-sectional area, see Tables B.4 to B.6 of Damasceno (1992). The measured supernate-suspension interface height values $l = l(t)$ are plotted in Figure 11. All of these nine runs include a portion in which the settling velocity is nearly constant. We have calculated least-squares straight-lined approximations these portions. The slopes of these segments are the velocities u_0 listed in the table included in Figure 11.

To estimate values of f_{bk} from these velocities, we recall that discontinuities of solutions to the first-order conservation law

$$\frac{\partial \phi}{\partial t} + \frac{\partial f_{\text{bk}}(\phi)}{\partial x} = 0,$$

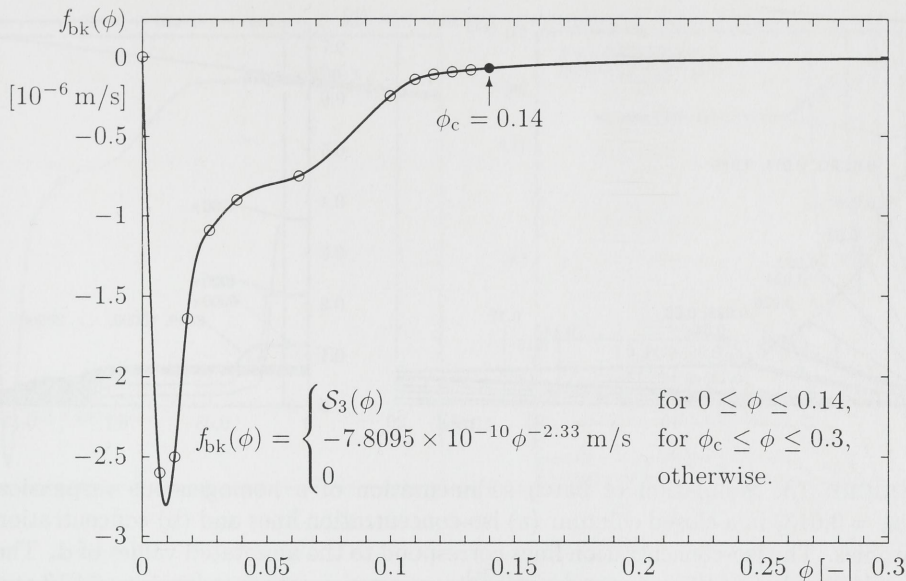


FIGURE 12. Kynch batch flux density function $f_{\text{bk}}(\phi)$ for a calcium carbonate suspension (Damasceno, 1992). The open circles denote the data points of the interpolating cubic spline function $\mathcal{S}_3(\phi)$.

to which (13) or (14) reduces for $S = \text{const.}$, $Q_D \equiv 0$ and wherever $\phi \leq \phi_c$, travel at the speed $\sigma(\phi^-, \phi^+)$ given by the Rankine-Hugoniot condition (40). Consequently, with $\phi^- = \phi_0$ and $\phi^+ = 0$, the settling rate or suspension-supernate interface velocity u_0 of an initially homogeneous suspension of concentration ϕ_0 satisfies $u_0 \approx \sigma(\phi_0, 0) = f_{\text{bk}}(\phi_0)/\phi_0$. Thus the values $\phi_0 u_0$ computed from the experimental data (see the last column of the table in Figure 11) represent approximate values of $f_{\text{bk}}(\phi_0)$. It turns out that these values are within the same range for all runs. This observation suggests that f_{bk} has a local minimum between $\phi = 0.007$ and 0.013 . In fact, we have chosen here the flux density function f_{bk} as the unique piecewise cubic interpolating natural spline function \mathcal{S}_3 satisfying $\mathcal{S}_3(0) = 0$, $\mathcal{S}_3(0.007) = -2.6 \times 10^{-6}$ m/s and $\mathcal{S}_3(0.013) = -2.5 \times 10^{-6}$ m/s in order to be consistent with the table of Figure 11,

$$\mathcal{S}_3(0.14) = -7.8095 \times 10^{-10} \times 0.14^{-2.33} \text{ m/s} = -7.6233 \times 10^{-8} \text{ m/s}$$

to connect continuously with the segment of f_{bk} given by (47), and $\mathcal{S}_3(\phi_i) = G_i$ for nine particular values $\phi_i \in [0.02, 0.12]$, $i = 3, \dots, 11$, where the choice of these points is discussed below.

The segment of f_{bk} for ϕ between 0.013 and 0.14 is, of course, speculative, since no settling experiments with initial concentrations in this range have been conducted. However, some qualitative information is available from the experimental settling plots of Figure 11. For example, consider the run with $\phi_0 = 0.013$ and $l(0) = 0.75$ m. An upper bound of the sediment height x_c results from the assumption that all the solids are contained in the sediment; and that the sediment is of the uniform concentration $\phi = \phi_c$. Consequently, for this run

$$x_c \leq \frac{L\phi_0}{\phi_c} = \frac{0.75 \text{ m} \times 0.013}{0.14} = 0.0696 \text{ m}.$$

However, the last data point \diamond plotted in Figure 11 corresponds to a supernate-suspension height of 0.097 m attained at $t = 7871$ s (Table B.6 of Damasceno, 1992).

Assuming that 0.14 is the correct value of ϕ_c , we conclude that at that time the critical time t_c , at which the supernate-suspension and suspension-sediment interfaces merge, is not yet reached. Therefore the curved shape of the supernate-suspension interface for the run considered represents a curved kinematic shock, that is a discontinuity separating varying but subcritical concentration

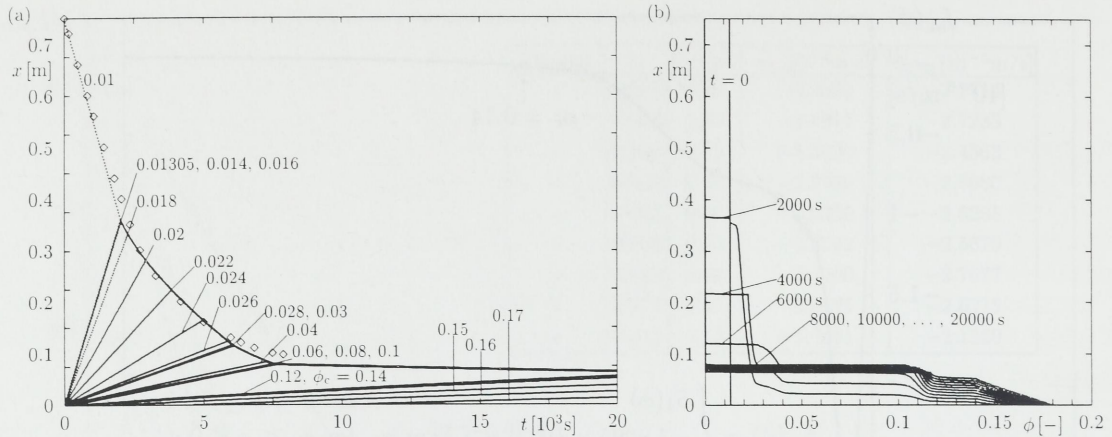


FIGURE 13. Simulation of batch sedimentation of a homogeneous suspension ($\phi_0 = 0.013$) in a closed column: (a) iso-concentration lines and (b) concentration profiles. The iso-concentration lines correspond to the annotated values of ϕ . The symbols \diamond denote the measured supernate-suspension interface for $\phi_0 = 0.013$ and $l(0) = 0.75$ m, see Fig. 11.

values from the clear liquid zone where $\phi = 0$. As is well known from the incompressible (kinematic) case, where $\sigma_e \equiv 0$, these curved shocks are related to the presence of lower rarefaction waves, which are zones of continuous (vertical) transitions between concentration values located between the rising sediment and the bulk suspension at its initial concentration, see Bustos et al. (1999) and Bürger and Tory (2000) for details. A necessary requirement for the presence of a lower rarefaction wave, say ranging from a concentration value ϕ_1 to ϕ_2 , is that $f''_{bk}(\phi) < 0$ for $\phi_1 \leq \phi \leq \phi_2$, as can be inferred from the construction of the settling plot as an entropy solution using the method of characteristics (Bustos and Concha, 1988; Bustos et al., 1999). These considerations have led us to choose the control points in such a way that the resulting segment of \mathcal{S}_3 between 0.013 and (roughly) 0.05. Similar arguments were used by Diplas and Papanicolaou (1997) for determining the flux density function f_{bk} for a settling experiment by Tiller and Khatib (1984), see also Garrido et al. (2001), and by Bürger et al. (2001) in order to determine the model function for a kaolin suspension. Flux density functions of similar shape (with three inflection points) were also used by Scott (1968) and Font et al. (1998).

The graph of the resulting flux density function f_{bk} , as well as the data points determining the spline function \mathcal{S}_3 , are plotted in Figure 12.

5.2.2. Batch sedimentation in a closed cylindrical vessel. To show that the mathematical model, complemented by the choices of the functions f_{bk} and σ_e , leads to a reasonable approximation of the observed settling behaviour, the numerical algorithm outlined in Section 3 is employed to simulate the batch sedimentation ($Q_D \equiv 0$) of a suspension of initially homogeneous concentration $\phi_0 = 0.013$ in a column of constant cross-sectional area ($S \equiv \text{const.}$) and height $L = 0.75$ m. The spatial discretization parameter is $J = 600$. Figure 13 displays the numerical result both as a settling plot, showing iso-concentration lines, and as a sequence of concentration profiles. We observe that due to the construction of f_{bk} , the simulated supernate-suspension interface settles slightly faster than the observed, and that the curved supernate-suspension interface is well reproduced. Furthermore, the compression zone is relatively thin.

5.3. Steady state computations. Calcium carbonate suspensions are frequently used for laboratory sedimentation, thickening and filtration experiments. On the other hand, the size (height and diameter) of laboratory equipment is usually smaller than are thickeners used in industrial plants. For example, Freitas et al. (2000) report experiments with three different laboratory-scale conical and cylindrical continuous thickeners of approximately 20 cm height. We here calculate

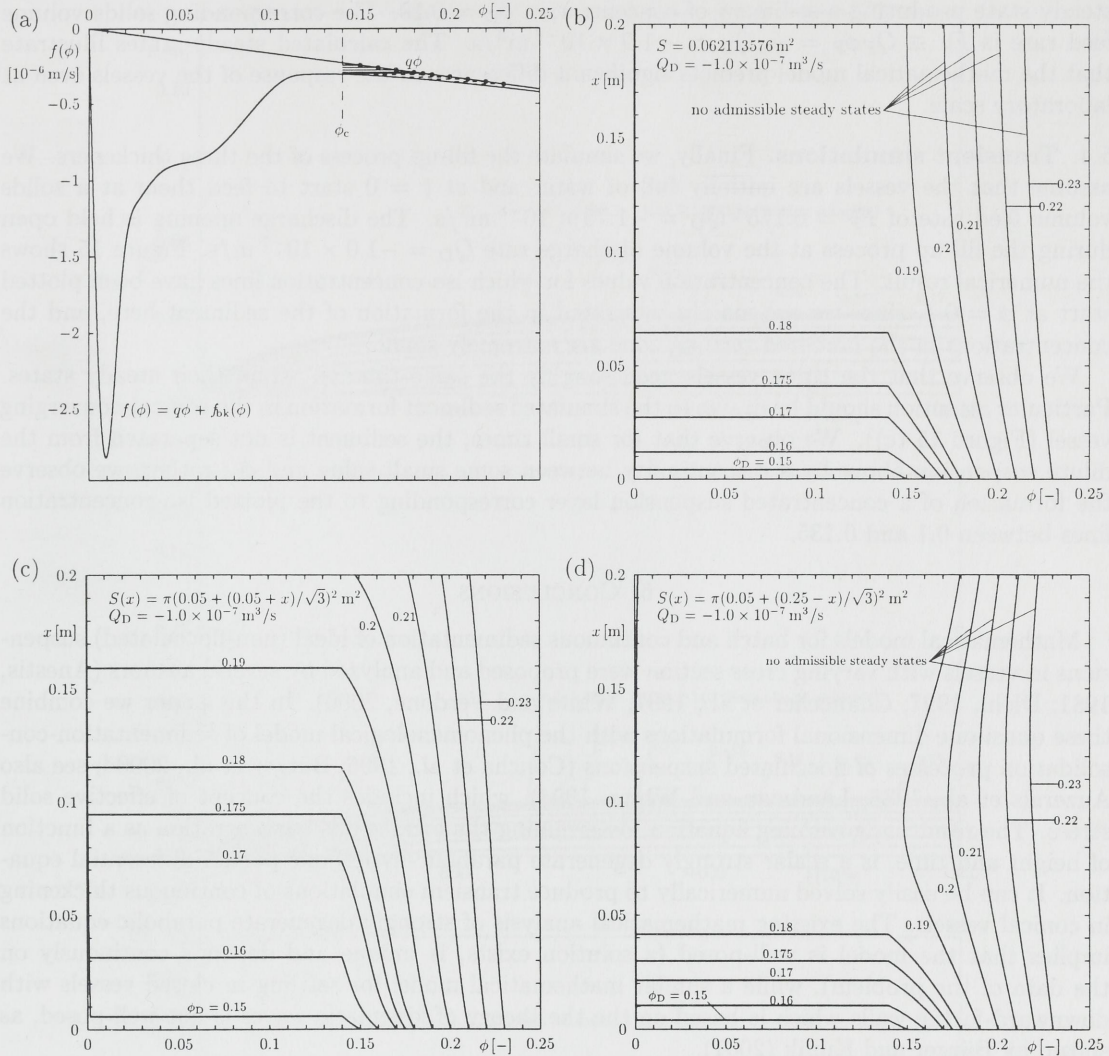


FIGURE 14. Steady states for continuous thickening of a calcium carbonate suspension in three different cylindrical and conical laboratory vessels. (a) Flux plot for the cylindrical vessel. The horizontal solid and dashed lines correspond to admissible and inadmissible steady states, respectively. Steady concentration profiles in (b) a cylindrical vessel, and (c,d) conical vessels with (c) upward-facing and (d) downward-facing lateral wall. The profiles in diagram (c) for $\phi_D \geq 0.2$ are part of steady states with sediment heights greater than the vessel height.

first steady state profiles for three different ideal conical thickeners. The height is always $L = 0.2$ m and the volume of the three vessels is identical. The conical vessels are assumed to be formed by a section of a cone of opening angle 60° cut in distances of 0.1366 m and 0.3366 m to its vertex, where shape of the conical-diverging vessel (with the cross-sectional area increasing downwards) is obtained by turning the conical-converging vessel upside down. Thus we consider (a) a cylindrical thickener with constant cross-sectional area $S = 0.062113576 \text{ m}^2$, (b) a conical-converging thickener with $S(x) = \pi(0.05 + (0.05 + x)/\sqrt{3})^2 \text{ m}^2$ and (c) a conical-diverging thickener with $S(x) = \pi(0.05 + (0.25 - x)/\sqrt{3})^2 \text{ m}^2$. For a given volume discharge rate $Q_D = -1.0 \times 10^{-7} \text{ m}^3/\text{s}$, steady states for several discharge concentrations ϕ_D have been calculated, see Figure 14, which is similar to Figure 6. We here observe that only the conical-converging vessel is able to operate at

steady state producing a sediment of concentration $\phi_D = 0.19$. The corresponding solids volume feed rate is $F_F \equiv Q_F \phi_F = \phi_D Q_D = -1.9 \times 10^{-8} \text{ m}^3/\text{s}$. The calculated steady states illustrate that the mathematical model predicts significant differences in the response of the vessels even at laboratory scale.

5.4. Transient simulations. Finally, we simulate the fill-up process of the three thickeners. We assume that the vessels are initially full of water and at $t = 0$ start to feed them at a solids volume feed rate of $F_F = 0.175 \cdot Q_D = -1.75 \times 10^{-8} \text{ m}^3/\text{s}$. The discharge opening is held open during the fill-up process at the volume discharge rate $Q_D = -1.0 \times 10^{-7} \text{ m}^3/\text{s}$. Figure 15 shows the numerical result. The concentration values for which iso-concentration lines have been plotted start at $\phi = 0.1$, since we are mainly interested in the formation of the sediment here, and the concentrations in the hindered settling zone are extremely small.

We observe that the three vessels need roughly the same time to attain their steady states. Particular attention should be drawn to the simulated sediment formation in the conical-converging vessel (Figure 15 (c)). We observe that for small times, the sediment is not separated from the dilute suspension above by a discontinuity between some small value and ϕ_c ; rather, we observe the formation of a concentrated suspension layer corresponding to the plotted iso-concentration lines between 0.1 and 0.135.

6. CONCLUSIONS

Mathematical models for batch and continuous sedimentation of ideal (non-flocculated) suspensions in vessels with varying cross section were proposed and analyzed by several authors (Anestis, 1981; Diehl, 1997; Chancelier et al., 1997; White and Verdone, 2000). In this paper we combine these quasi-one dimensional formulations with the phenomenological model of sedimentation-consolidation processes of flocculated suspensions (Concha et al., 1996; Bürger et al., 2000d; see also Auzeais et al., 1988; Landman and White, 1994), which includes the concept of effective solid stress. The resulting governing equation, determining the local solids concentration as a function of height and time, is a scalar strongly degenerate parabolic-hyperbolic partial differential equation. It can be easily solved numerically to produce transient simulations of continuous thickening in conical vessels. The existing mathematical analysis of strongly degenerate parabolic equations implies that the model is well-posed (a solution exists, is unique and depends continuously on the data of the problem), while a similar mathematical model for settling in closed vessels with downward-facing walls which is based on the theory of kinematic waves is not well-posed, as shown by Bürger and Kunik (2001).

Traditional methods of thickener design, such as those by Coe and Clevenger (1916), Talmage and Fitch (1955) and Adorján (1975, 1977) and as reviewed by Concha and Barrientos (1993), Schubert (1998) or in Chapter 11 of Bustos et al. (1999), usually refer to cylindrical settling tanks. The parameters determined are usually the unit area of the equipment needed to treat a given solids handling rate and the height of the equipment necessary to accommodate the sediment. To this end, properties of steady state concentration profiles, determined from the ordinary differential equation obtained from the governing partial differential equation in the stationary case under continuous flow conditions, can be utilized. Such calculations were performed for a large number of materials by Tiller and Chen (1988), whose consolidation model is equivalent to ours in the relevant zone determining the thickener height, i.e. in the compression zone, where $\phi > \phi_c$.

It should also be interesting to go even a step further and ask for the optimal area function $S(x)$ which minimizes the thickener volume for a given material and operating conditions (we here only demonstrate that a particular conical ‘solution’ outperforms the cylindrical one). This should also open new possibilities of design for units known as ‘deep thickeners’ (Chandler, 1982; Tiller and Targ, 1995) or ‘deep cone thickeners’ (Rushton et al., 2000).

In the transient numerical examples of Section 5.1.3 the initial steady state is attained more rapidly in a conical than in a comparable cylindrical thickener. This is in qualitative agreement with experimental observations stated elsewhere (Freitas et al., 2000), and the numerical algorithm should be employed to examine systematically the dynamics of continuous thickening in non-cylindrical vessels.

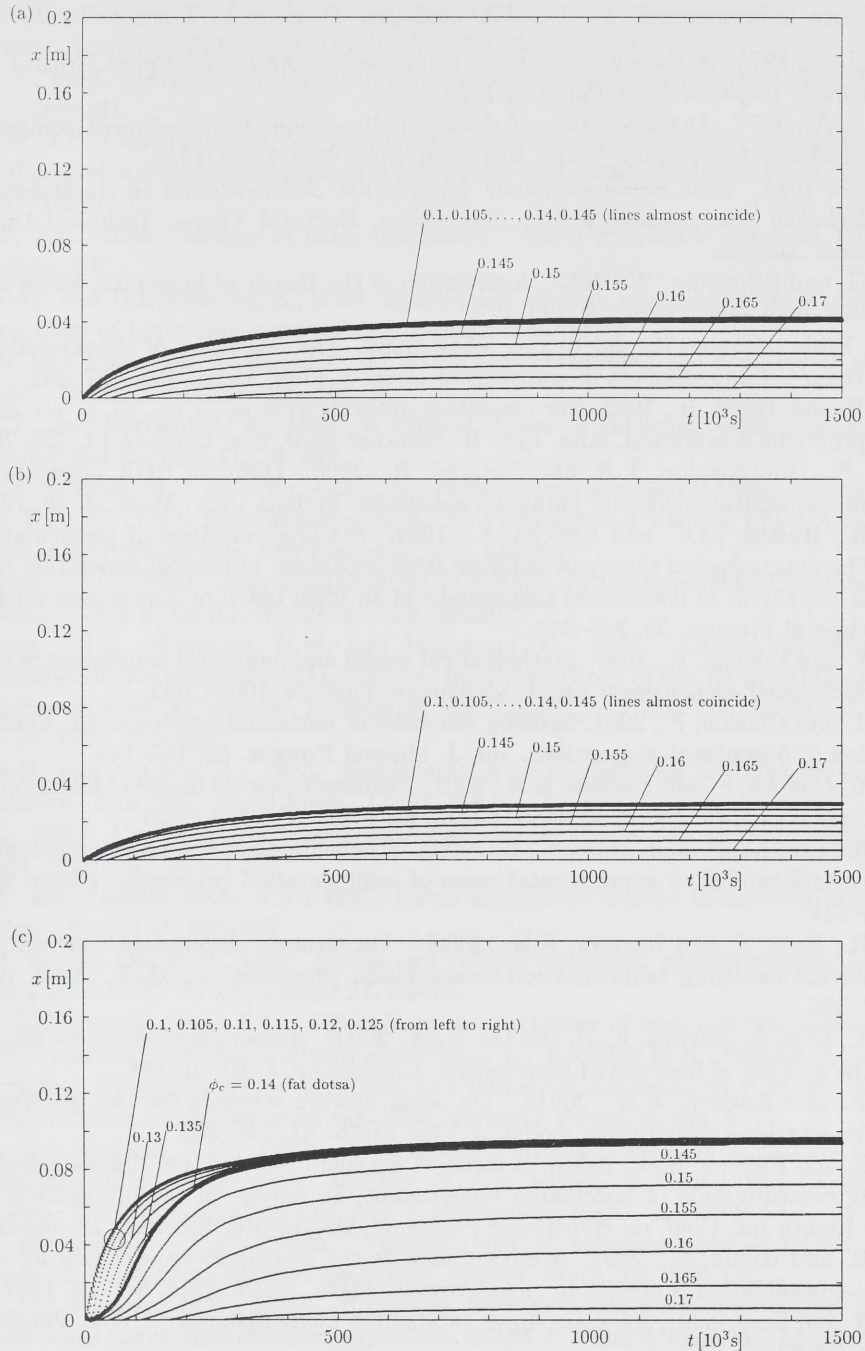


FIGURE 15. Simulation of filling up (a) the cylindrical, (b) the diverging and (c) the converging conical continuous thickeners (of Figure 14) at solids volume feed rate $F_F = 0.175 \cdot Q_D = -1.75 \times 10^{-8} \text{ m}^3/\text{s}$. The discretization parameter is $J = 600$.

ACKNOWLEDGEMENTS

We acknowledge support by the Collaborative Research Programme (Sonderforschungsbereich) 404 "Mehrfeldprobleme in der Kontinuumsmechanik" at the University of Stuttgart.

REFERENCES

- Adorján, L.A., 1975. A theory of sediment compression. *XI International Mineral Processing Congress, Cagliari, Italy*, Paper 11:1–22.
- Adorján, L.A., 1977. Determination of thickener dimensions from sediment compression and permeability test results. *Trans. Inst. Min. Met.* 85, C157–C163.
- Anestis, G., 1981. *Eine eindimensionale Theorie der Sedimentation in Absetzbehältern veränderlichen Querschnitts und in Zentrifugen*, Doctoral Thesis, Technical University of Vienna, Austria.
- Anestis, G. and Schneider, W., 1983. Application of the theory of kinematic waves to centrifugation. *Ingenieur-Archiv* 53, 399–407.
- Auzerais, F.M., Jackson, R. and Russel, W.B., 1988. The resolution of shocks and the effects of compressible sediments in transient settling. *J. Fluid Mech.* 195, 437–462.
- Bénilan, P. and Touré, H., 1995. Sur l'équation générale $u_t = a(\cdot, u, \phi(\cdot, u))_x + v$ dans L^1 . II. Le problème d'évolution. *Ann. Inst. H. Poincaré Anal. Non Linéaire* 12, 727–761.
- Bouchut, F., Guarguaglini, F.R. and Natalini, R., 2000. Diffusive BGK approximations for nonlinear multidimensional parabolic equations. *Indiana Univ. Math. J.* 49, 723–749.
- Bürger, R., Bustos, M.C. and Concha, F., 1999. Settling velocities of particulate systems: 9. Phenomenological theory of sedimentation processes: numerical simulation of the transient behaviour of flocculated suspensions in an ideal batch or continuous thickener. *Int. J. Mineral Process.* 55, 267–282.
- Bürger, R. and Concha, F., 1998. Mathematical model and numerical simulation of the settling of flocculated suspensions. *Int. J. Multiphase Flow* 24, 1005–1023.
- Bürger, R. and Concha, F., 2001. Settling velocities of particulate systems: 12. Batch centrifugation of flocculated suspensions. *Int. J. Mineral Process.* 63, 115–145.
- Bürger, R., Concha, F. and Karlsen, K.H., 2001. Phenomenological model of filtration processes: 1. Cake formation and expression. *Chem. Eng. Sci.* 56, 4537–4553.
- Bürger, R., Concha, F. and Tiller, F.M., 2000a. Applications of the phenomenological theory to several published experimental cases of sedimentation processes. *Chem. Eng. J.* 80, 105–117.
- Bürger, R., Evje, S. and Karlsen, K.H., 2000b. On strongly degenerate convection-diffusion problems modeling sedimentation-consolidation processes. *J. Math. Anal. Appl.* 247, 517–556.
- Bürger, R., Evje, S., Karlsen, K.-H. and Lie, K.-A., 2000c. Numerical methods for the simulation of the settling of flocculated suspensions. *Chem. Eng. J.* 80, 91–104.
- Bürger, R. and Karlsen, K.H., 2001a. On some upwind schemes for the phenomenological sedimentation-consolidation model. *J. Eng. Math.* 41, 145–166.
- Bürger, R. and Karlsen, K.H., 2001b. A strongly degenerate convection-diffusion problem modeling centrifugation of flocculated suspensions. To appear in the proceedings volume of the Eighth Int. Conf. on Hyperbolic Problems, Magdeburg, February 28–March 3, 2000.
- Bürger, R. and Kunik, M., 2001. A critical look at the kinematic-wave theory for sedimentation-consolidation processes in closed vessels. *Math. Meth. Appl. Sci.* 24, 1257–1273.
- Bürger, R. and Tory, E.M., 2000. On upper rarefaction waves in batch settling. *Powder Technol.* 108, 74–87.
- Bürger, R. and Wendland, W.L., 1998a. Entropy boundary and jump conditions in the theory of sedimentation with compression. *Math. Meth. Appl. Sci.* 21, 865–882.
- Bürger, R. and Wendland, W.L., 1998b. Existence, uniqueness, and stability of generalized solutions of an initial-boundary value problem for a degenerating quasilinear parabolic equation. *Math. Anal. Appl.* 218, 207–239.
- Bürger, R., Wendland, W.L. and Concha, F., 2000d. Model equations for gravitational sedimentation-consolidation processes. *Z. Angew. Math. Mech.* 80, 79–92.
- Bustos, M.C. and Concha, F., 1988. On the construction of global weak solutions in the Kynch theory of sedimentation. *Math. Meth. Appl. Sci.* 10, 245–264.

- Bustos, M.C., Concha, F., Bürger, R. and Tory, E.M., 1999. Sedimentation and Thickening. Kluwer Academic Publishers, Dordrecht, The Netherlands.
- Carrillo, J., 1999. Entropy solutions for nonlinear degenerate problems. Arch. Rat. Mech. Anal. 147, 269–361.
- Chancelier, J.P., Cohen de Lara, M., Joannis, C. and Pacard, F., 1997. New insights in dynamic modeling of a secondary settler—I. Flux theory and steady-states analysis, Wat. Res. 31, 1847–1856.
- Chandler, J.L., 1982. Design of deep thickeners. World Filtration Congress III, Filtration Society, UK.
- Chen, G.-Q. and DiBenedetto, E., 2000. Stability of entropy solutions to the Cauchy problem for a class of hyperbolic-parabolic equations. Preprint.
- Coe, H.S. and Clevenger, G.H., 1916. Methods for determining the capacity of slimesettling tanks. Trans. AIME 55, 356–385.
- Concha, F. and Barrientos, A., 1993. A critical review of thickener design methods, KONA Powder and Particle 11, 79–104.
- Concha, F., Bustos, M.C. and Barrientos, A., 1996. Phenomenological theory of sedimentation. In: Tory, E. (Ed.), Sedimentation of Small Particles in a Viscous Fluid, Computational Mechanics Publications, Southampton, UK, 51–96.
- Damasceno, J.J.R., 1992. Uma Contribuição ao Estudo do Espessamento Contínuo. Doctoral Thesis, COPPE/UFRJ, Rio de Janeiro, Brazil.
- Damasceno, J.J.R., Henrique, H.M. and Massarani, G., 1992. Análise do comportamento dinâmico de um espessador Dorr-Oliver. In: Proceedings of the III Meeting of the Southern Hemisphere on Mineral Technology, São Lourenço, Minas Gerais, Brazil, September 13–16, 1992, 675–689.
- Davis, R.H. and Acrivos, A., 1985. Sedimentation of noncolloidal particles at low Reynolds numbers. Ann. Rev. Fluid Mech. 17, 91–118.
- Diehl, S., 1997. Dynamic and steady-state behavior of continuous sedimentation. SIAM J. Appl. Math. 57, 991–1018.
- Diplas, P. and Papanicolaou, A.N., 1997. Batch analysis of slurries in zone settling regime. J. Environ. Eng. 123, 659–667.
- Engquist, B. and Osher, S., 1980. Stable and entropy satisfying approximations for transonic flow calculations. Math. Comp. 34, 45–75.
- Espedal, M.S. and Karlsen, K.H., 2000. Numerical solution of reservoir flow models based on large time step operator splitting algorithms. In: Espedal, M.S., Fasano, A. and Mikelić, A. (Eds.) Filtration in Porous Media and Industrial Applications (Cetraro, Italy, 1998). Lecture Notes in Mathematics vol. 1734, Springer-Verlag, Berlin, 9–77.
- Evje, S. and Karlsen, K.H., 1999a. Degenerate convection-diffusion equations and implicit monotone difference schemes. In: Fey, M. and Jeltsch, R. (Eds.) Hyperbolic Problems: Theory, Numerics, Applications, Vol. I. Birkhäuser, Basel, 285–294.
- Evje, S. and Karlsen, K.H., 1999b. Viscous splitting approximation of mixed hyperbolic-parabolic convection-diffusion equations. Numer. Math. 83, 107–137.
- Evje, S. and Karlsen, K.H., 2000. Monotone difference approximations of BV solutions to degenerate convection-diffusion equations. SIAM J. Numer. Anal. 37, 1838–1860.
- Eymard, R., Gallouët, T., Herbin, R. and Michel, A., 2000. Convergence of a finite volume scheme for nonlinear degenerate parabolic equations. Preprint.
- Font, R., García, P. and Pérez, M., 1998. Analysis of the variation of the upper discontinuity in sedimentation batch test. Sep. Sci. Technol. 33, 1487–1510.
- França, S.C.A., 2000. *Equações Constitutivas para a Sedimentação de Suspensões Flocculentas*. Doctoral Thesis, PEQ/COPPE, Federal University of Rio de Janeiro, Brazil.
- França, S.C.A., Massarani, G. and Biscaia Jr., E.C., 1999. Study on batch sedimentation—establishment of constitutive equations. Powder Technol. 101, 157–164.

- Freitas, K.A., Silva, T.A. and Damasceno, J.J.R., 2000. Espessadores cônico-cilíndricos: uma avaliação experimental. In: Giudici, R. and Guardani, R. (Eds.), *Anais do XXVII Congresso Brasileiro de Sistemas Particulados (XXVII ENEMP)*, EPUSP, São Paulo, Brazil, 2000, 87–93.
- Garrido, P., Bürger, R. and Concha, F., 2000. Settling velocities of particulate systems: 11. Comparison of the phenomenological sedimentation-consolidation model with published experimental results. *Int. J. Mineral Process.* 60, 213–227.
- Garrido, P., Concha, F. and Bürger, R., 2001. Application of the unified model of solid-liquid separation of flocculated suspensions to experimental results. In: da Luz, A.B., Soares, P.S.M., Torem, M.L. and Trindade, R.B.E. (Eds.), *Proceedings of the VI Southern Hemisphere Meeting on Mineral Technology*, Rio de Janeiro, Brazil, May 27–31, 2001, Vol. 1, CETEM/MCT, Rio de Janeiro, 117–122.
- Holden, H., Karlsen, K.H. and Lie, K.A., 2001. Operator splitting methods for degenerate convection-diffusion equations I: convergence and entropy estimates. In: *Stochastic Processes, Physics and Geometry: New Interplays. A Volume in Honor of Sergio Albeverio*. Amer. Math. Soc., to appear.
- Karlsen, K.H. and Ohlberger, M., 2001. A note on the uniqueness of entropy solutions of nonlinear degenerate parabolic equations. Preprint.
- Karlsen, K.H. and Risebro, N.H., 2000. On the uniqueness and stability of entropy solutions of nonlinear degenerate parabolic equations with rough coefficients. Preprint, Department of Mathematics, University of Bergen.
- Karlsen, K.H. and Risebro, N.H., 2001. Convergence of finite difference schemes for viscous and inviscid conservation laws with rough coefficients. *M2N Math. Model. Numer. Anal.* 35, 239–270.
- Kröner, D., 1997. *Numerical Schemes for Conservation Laws*. John Wiley & Sons Ltd., Chichester and Stuttgart.
- Kružkov, S.N., 1970. First order quasi-linear equations in several independent variables. *Math. USSR Sb.* 10, 217–243.
- Kynch, G.J., 1952. A theory of sedimentation. *Trans. Faraday Soc.* 48, 166–176.
- Landman, K.A. and White, L.R., 1994. Solid/liquid separation of flocculated suspensions. *Adv. Colloid Interf. Sci.* 51, 175–246.
- Mascia, C., Porretta, A. and Terracina, A., 2001. Nonhomogeneous Dirichlet problems for degenerate parabolic-hyperbolic equations. *Arch. Rat. Mech. Anal.*, to appear.
- Michaels, A.S. and Bolger, J.C., 1962. Settling rates and sediment volumes of flocculated Kaolin suspensions. *Ind. Eng. Chem. Fund.* 1, 24–33.
- Ohlberger, M. A posteriori error estimates for vertex centered finite volume approximations of convection-diffusion-reaction equations. *M2N Math. Model. Numer. Anal.* 35, 355–387.
- Quispe, J., Concha, F. and Toledo, P.G., 2000. Discrete sedimentation model for ideal suspensions. *Chem. Eng. J.* 80, 135–140.
- Resende, M.M., Henrique, H.M. and Damasceno, J.J.R., 1995. Um modelo para o estudo da operação de espessadores cônicos e cilíndricos. In: *Anais do XXII Encontro Nacional sobre Escoamento em Meios Porosos*, Florianópolis, SC, Brazil, 236–243.
- Richardson, J.F. and Zaki, W.N., 1954. Sedimentation and fluidization: Part I. *Trans. Instn. Chem. Engrs. (London)* 32, 35–53.
- Rouvre, E. and Gagneux, G., 1999. Solution forte entropique de lois scalaires hyperboliques-paraboliques dégénérées. *C. R. Acad. Sci. Paris Sér. I Math.* 329, 599–602.
- Rushton, A., Ward, A.S. and Holdich, R.G. (2000) *Solid-Liquid Filtration and Separation Technology*. Second Edition. Wiley-VCH, Weinheim, Germany.
- Schubert, H., 1998. Zur Auslegung von Schwerkrafteindickern/On the design of thickeners, *Aufber.-Techn.* 39, 593–606.
- Scott, K.J., 1968. Experimental study of continuous thickening of a flocculated silica slurry. *Ind. Eng. Chem. Fund.* 7, 582–595.
- Talmage, W.P. and Fitch, E.B., 1955. Determining thickener unit areas. *Ind. Eng. Chem.* 47, 38–41.

- Tiller, F.M. and Chen, W., 1988. Limiting operating conditions for continuous thickeners. *Chem. Eng. Sci.* 43, 1695-1704.
- Tiller, F.M. and Khatib, Z., 1984. The theory of sediment volumes of compressible, particulate structures. *J. Colloid Interf. Sci.* 100, 55-67.
- Tiller, F.M. and Leu, W.F., 1980. Basic data fitting in filtration. *J. Chin. Inst. Chem. Engrs.* 11, 61-70.
- Tiller, F.M. and Tarng, D., 1995. Try deep thickeners and clarifiers. *Chem. Eng. Prog.* 91 (March 1995), 75-80.
- Volpert, A.I., 2000. Generalized solutions of degenerate second-order quasilinear parabolic and elliptic equations. *Adv. Diff. Eqns.* 5, 1493-1518.
- Vol'pert, A.I. and Hudjaev, S.I., 1969. Cauchy's problem for degenerate second order quasilinear parabolic equations. *Math. USSR Sb.* 7, 365-387.
- White, D.A. and Verdone, N., 2000. Numerical modelling of sedimentation processes. *Chem. Eng. Sci.* 55, 2213-2222.
- Wu, Z. and Yin, J., 1989. Some properties of functions in BV_x and their applications to the uniqueness of solutions for degenerate quasilinear parabolic equations. *Northeast. Math. J.* 5, 395-422.

025d 01631



Depotbiblioteket



02sd 01 631

